Journal of Applied Analysis and Computation
Volume 14, Number 4, August 2024, 2283–2316
Website:http://www.jaac-online.com
DOI:10.11948/20230365

STUDIES ON THE INTERACTION MECHANISM BETWEEN THE MRNA VACCINE AGAINST SARS-COV-2 AND THE IMMUNE SYSTEM

Yuhao Shou[1] and Jie Lou[1,†]

Abstract Vaccines are an effective tool in the fight against infectious diseases. However, mathematical models of SARS-CoV-2 focus on the macroscopic situation, while articles on vaccines focus on effectiveness and safety. We develop four mathematical models to investigate the immune system and the microdynamics of antigens and viruses in individuals injected with mRNA vaccines. We first theoretically analyze the optimal model, calculate all equilibria, and prove that the disease-free equilibrium is globally asymptotically stable while the others are unstable. This suggests that after a certain period after vaccination, the infected cells and antigens will no longer exist in vivo and will be eliminated by the immune system over time or will die naturally. This theoretically proves the safety of the mRNA vaccines. Then, we use the differential algebra to analyze the structural identifiability of the models. We find that two of them are globally identifiable while the other two are unidentifiable, but once a certain parameter is fixed, then they are identifiable as well. To select the optimal model among four models, we use the Affine Invariant Ensemble Markov Chain Monte Carlo algorithm for data fitting and parameter estimation. We find that the roles of memory cells in killing infected cells and promoting immune cells and neutralizing antibodies in the process of mRNA vaccination are not significant and can be ignored in the modeling. On the other hand, the innate immunity of the human body plays an important role in this process. In addition, we also analyze the practical identifiability of the parameters of the optimal model. The results show that even if the structure of the system is globally identifiable, it does not ensure that all the parameters are practically identifiable. After random sampling and simulating the four unidentifiable parameters, we find that only two variables, infected cells II and antibodies, are sensitive to these unidentifiable parameters, but the results are still within acceptable ranges. This suggests that our fitting results are generally reliable. Finally, we simulate multiple booster injections and find that booster injections are indeed effective in maintaining antibody levels in vivo, which could otherwise gradually die off over time. Therefore, booster injections are beneficial to help the human body increase and maintain immunity.

Keywords MRNA vaccine against SARS-CoV-2, mathematical model, parameter identification, GWMCMC.

MSC(2010) 92D30, 92D40.

[†]The corresponding author.
[1]Department of Mathematics, Shanghai University, 99 Shangda Road Shanghai, 200444, China
Email: 18516678794@163.com(Y. Shou), jie_lou@shu.edu.cn(J. Lou)

1. Introduction

The discovery of SARS-CoV-2 at the end of 2019 has already caused significant health risks and economic burdens in human life over the past three years. Although the virulence of the viruses is decreasing, we still need to emphasize protection against the viruses. Since vaccination is an important way to prevent and control the spread of epidemics as well as to reduce symptoms and mortality in patients, it is medically important to investigate the effects of vaccines on the human immune system.

Vaccines against polio, encephalitis B, influenza, rabies, and HFMD are usually inactivated vaccines. The mechanism is to kill or inactivate the infectious viruses by some physical or chemical treatment, but keep the viruses intact, and then inject them in vivo. Although they are intact viruses, they do not infect healthy cells. Once the body's immune system recognizes these viruses, it responds and develops a memory of them.

In the 1990s, scientists discovered that target proteins can be successfully detected after injecting mRNAs into mice [24]. Subsequent experiments have shown that it is possible to inject viral mRNAs in vivo, guiding the cells to synthesize the corresponding antigens, thereby inducing a specific immune response. Specifically, the mRNA vaccine injects the mRNAs of the desired antigens, rather than the antigens themselves. Ribosomes in the cells will translate these mRNAs into the corresponding proteins, which are the antigens. Once circulating in the bloodstream, these antigens trigger a response from the immune system. In contrast to traditional inactivated vaccines, these antigens are active, so that they can infect target cells and thus induce both humoral immunity and cellular immunity simultaneously.

The antigens of the mRNA vaccine against SARS-CoV-2 are the spike proteins (also known as the S proteins) on the surface of the viruses. In an intact virus, the S proteins bind with the ACE2 receptors on the surface of human cells to allow the viral mRNAs to enter the cell [11], thus allowing the virus to proliferate. Therefore, if the vaccines contain only the mRNAs of the S proteins but not the viral mRNAs, they will infect the target cells but will not be able to proliferate the viruses themselves, thus ensuring the safety of the vaccines. In addition, we can flexibly change and optimize the mRNA sequence to produce vaccines to counteract viral mutations.

In 2020, two mRNA vaccines against SARS-CoV-2 developed by Modena and Pfizer/BioNTech were licensed and marketed for the first time for emergency use. This is the first time that mRNA vaccines have been mass-vaccinated in the world. Moderna announced Phase 1 clinical trial results of its mRNA vaccine mRNA-1273 against SARS-CoV-2 in July 2020 [18], and Pfizer/BioNTech announced Phase 1/2 clinical trial results of their vaccine BNT162b2 in August of the same year [29], and preliminary results showed that the vaccines could produce more antibodies than patients recovering from natural infection and that the vaccines were safe. The efficacy and safety of mRNA-1273 was further studied by L. R. Baden et al. [4]. The efficacy and safety of BNT162b2 was further studied by F. P. Polack et al. [31]. The effectiveness of a lower dose of mRNA-1273 was studied by J. Mateus et al. [25]. The Sheba Medical Center in Israel evaluated the efficacy of a fourth booster dose of both vaccines against the Omicron variant [32]. All these results illustrate the effectiveness and importance of mRNA vaccines for the prevention of SARS-CoV-2

from different perspectives.

The mRNA vaccine was urgently introduced as a result of the epidemic. Is it really safe and effective in preventing SARS-CoV-2? And how necessary is a booster shot? The public has been skeptical about this. Therefore, we develop a nonlinear dynamics model and simulate virtual experiments to investigate this issue. Using the nonlinear system theory to research the interaction of the immune system with foreign matter, such as viruses or bacteria, has been shown to have great practical significance [15, 20, 33, 37]. However, not many studies have been conducted on the dynamics of the mRNA vaccine against SARS-CoV-2 in vivo and the dynamics of SARS-CoV-2 in vaccinated individuals. In general, due to the complexity of the immune system, we usually simplify the process by dividing the research objects into four groups. The first group consists of antigens, including invading viruses and bacteria, as well as tumor antigens and viral vaccines, which are spontaneously transformed into cancer cells from normal cells in vivo; the second group consists of immune cells, such as T cells, B cells, and macrophages; the third group consists of immune molecules, such as lymphokines, interleukins, interferons, and tumor necrosis factors; and the last group consists of the major histocompatibility antigens and autoantigens. We will try to use mathematical tools to describe the complex non-linear interactions among them (or among some of them) to study the complex behaviors in immune response and immunoregulation and the effects of various factors on these behaviors.

The main structure of the rest is organized as follows. We establish the differential equations according to the characteristics of the immune system and the mRNA vaccines and then theoretically analyze them in Section 2. The structural identifiability of all the models is discussed in Section 3. The data fitting and model selection are carried out for the clinical data in Section 4. The practical identifiability of the optimal model is analyzed in Section 5. The sensitivity analysis of parameters is analyzed and the virtual experiments of the optimal model are simulated in Section 6. Finally, we discuss the results of our model in Section 7.

2. Mathematical models

It is widely known that different assumptions about the interactions between the viruses or vaccines and the components of the immune system in the host can lead to different mathematical models. According to the mechanisms of the mRNA vaccine and the human immune system, we first develop the following differential equation model to characterize the interaction between them. Based on it, assuming that some of the immune responses can be ignored, we can obtain the other three models which are more concise.

The diagram of the basic dynamics model (we call it the full model) is shown in Figure 1. The variables of the model include target cells that can be infected by the mRNAs of the S proteins in vaccines (I_1), target cells that can be infected by the antigens (I_2), antigens (S), $CD8^+$ T cells (T_k), $CD4^+$ T cells (T_h), B cells (B), antibodies (A), memory $CD8^+$ T cells (T_{km}), memory $CD4^+$ T cells (T_{hm}), and memory B cells (B_m). The system (2.1) and the system (2.2) show the dynamics of the humoral immunity and the cellular immunity induced by vaccines of the full model. The biological meanings of each term in the equations are shown in the appendixes (see Appendix A).

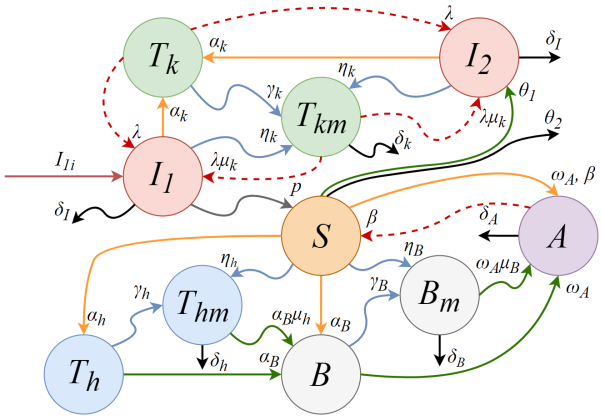

Figure 1. Dynamics of the mRNA Vaccination.

1. Humoral Immunity

$$\begin{cases} \dfrac{dS}{dt} = pI_1 - \beta SA - (\theta_1 + \theta_2)S, \\ \dfrac{dT_h}{dt} = \omega_h T_h(\pi_h - T_h) + \alpha_h S, \\ \dfrac{dB}{dt} = \omega_B B(\pi_B - B) + \alpha_B S(T_h + \mu_h T_{hm}), \\ \dfrac{dA}{dt} = \omega_A S(B + \mu_B B_m) - \beta SA - \delta_A A, \\ \dfrac{dT_{hm}}{dt} = \gamma_h T_h + \eta_h T_{hm} S - \delta_h T_{hm}, \\ \dfrac{dB_m}{dt} = \gamma_B B + \eta_B B_m S - \delta_B B_m. \end{cases} \tag{2.1}$$

2. Cellular Immunity

$$\begin{cases} \dfrac{dI_1}{dt} = -\lambda I_1(T_k + \mu_k T_{km}) - \delta_I I_1, & t \neq \tau_i (i = 1, 2, \ldots), \\ \dfrac{dI_2}{dt} = \theta_1 S - \lambda I_2(T_k + \mu_k T_{km}) - \delta_I I_2, \\ \dfrac{dT_k}{dt} = \omega_k T_k(\pi_k - T_k) + \alpha_k(I_1 + I_2), \\ \dfrac{dT_{km}}{dt} = \gamma_k T_k + \eta_k T_{km}(I_1 + I_2) - \delta_k T_{km}. \end{cases} \tag{2.2}$$

Obviously, the system (2.1) and the system (2.2) respectively characterize the two forms of immunity induced by the mRNA vaccine. One part is the humoral immunity involving the $CD4^+$ T cells, the B cells, the memory $CD4^+$ T cells, the memory B cells, and the neutralizing antibodies (system (2.1)). Like traditional inactivated vaccines, they are stimulated to proliferate by antigens free in the blood and are eventually neutralized by the neutralizing antibodies. The other part is the cellular immunity (system (2.2)) consisting of the $CD8^+$ T cells and the memory

Table 1. Sub-models.

Model	Assumption	Biological Meaning
Model 1	Full model	/
Model 2	$\theta_2 = 0$	Ignoring the killing of antigens by the innate immune system
Model 3	$\mu_i = 0 \ \ (i = k, h, B)$	Ignoring the killing of infected cells and the promotion of immune cells and neutralizing antibodies by memory cells
Model 4	$\theta_2, \mu_i = 0 \ \ (i = k, h, B)$	Ignoring the killing of infected cells and antigens by the innate immune system and memory cells

$CD8^+$ T cells. This is the advantage of mRNA vaccines over regular inactivated vaccines.

Based on the mechanism of mRNA vaccines, the full model (system (2.1) & (2.2)) contains three more concise sub-models under different biological assumptions. Table 1 lists four models based on different biological assumptions. For example, **Model 3** assumes that the parameters $\mu_i = 0 \ \ (i = k, h, B)$ in the full model, i.e., it assumes that the roles of memory cells in killing infected cells and promoting immune cells and neutralizing antibodies can be ignored. Of the four models, **Model 4** is the most concise, while ignoring the roles of both memory cells and the innate immune system in killing infected cells and antigens.

It is easy to see that none of the four models in Table 1 based on different biological assumptions has an infection equilibrium whose variables are all positive, and all of them have 8 disease-free equilibria (see Appendix A). We have obtained the following theorem about the stabilities of the 8 disease-free equilibria.

Theorem 2.1. *In the case of a single vaccination, the disease-free equilibrium of four systems of vaccination* **Model 1-Model 4**

$$\begin{aligned}&\boldsymbol{E_1}(I_1, I_2, S, T_k, T_h, B, A, T_{km}, T_{hm}, B_m)\\ &= \left(0, 0, 0, \pi_k, \pi_h, \pi_B, 0, \frac{\gamma_k \pi_k}{\delta_k}, \frac{\gamma_h \pi_h}{\delta_h}, \frac{\gamma_B \pi_B}{\delta_B}\right)^T\end{aligned}$$

is unconditionally globally asymptotically stable, while the other equilibria $\boldsymbol{E_i}(i = 2, \ldots, 8)$ *are unstable.*

The details of the proof are shown in the last chapter of the paper (see Appendix A). In fact, **Model 2**, **Model3** and **Model 4** are obtained from **Model 1** with some cuts. Take Model 3 as an example, since the memory immune cells T_{km}, T_{hm}, B_m are not involved in the immunization process, we can ignore them in the proof. Therefore, the expressions of the equilibria $E_i, i = 1, 2, \ldots, 8$ and the proof are more concise. Here, we only show the proof of the most complex sub-model **Model 1**. The proofs of the other three sub-models are the simplified versions of it, so we do not repeat them. This theorem implies that the mRNA vaccines are safe to some extent because there is no risk that a vaccinated individual will become infected with the viruses as a result of vaccination. This result also suggests that the level of antibodies will decrease with time until antibodies are completely eliminated. Multiple vaccinations may be necessary to maintain a certain level of antibodies in the absence of the viruses. We will prove this hypothesis through numerical simulations later.

3. Identifiability analysis of models

We collect the data of CD8$^+$ T cells T_k, CD4$^+$ T cells T_h, neutralizing antibodies A, memory CD8$^+$ T cells T_{km}, memory CD4$^+$ T cells T_{hm} and memory B cells B_m in individuals injected with mRNA vaccines mRNA-1273 or BNT162b2 from the literature [13, 22, 39]. Details about these data can be found in Appendix B. We plan to use these clinical data to estimate the parameters of each of the four models mentioned above (see Table 1) and do model selection. To ensure the reliabilities of parameter estimation and model selection, first, we need to analyze the structural identifiability of the models.

Structural identifiability analysis assumes that the measured data are ideally free of interferences and errors. The structure of a model is said to be unidentifiable if an infinite number of combinations of parameters can be fitted to the data. The structure of a model is said to be locally identifiable if only a finite number of parameter combinations can be fitted to the data. The structure of a model is said to be globally identifiable if there is only one unique combination of parameters that can fit the data. For the data observed, assuming that they are free of noise errors, the predictions of the unidentifiable and locally identifiable cases can be greatly different, even though models with different parameter combinations can fit the observations well. Therefore, the fact that the structure of a model is identifiable from the data is a prerequisite for the reliability of the parameter estimation. In contrast, although the structure is found to be unidentifiable, even if the parameter estimation fails, we can reveal useful information about the relationship between the parameters. This makes the structural identifiability analysis of models an important factor to consider in immunological modeling [9]. However, structural identifiability analysis has been neglected in the majority of modeling studies in systematic biology.

To determine whether the parameters of the four built models are identifiable in the ideal case (noise-free data), we use differential algebra to test the structural identifiability of the models, and the following are the strict definitions of structural identifiability [27]:

Definition 3.1. Global identifiability: A system structure is said to be globally identifiable if for any admissible input $\boldsymbol{u}(t)$ and any two parameter vectors $\boldsymbol{\theta_1}$ and $\boldsymbol{\theta_2}$ in the parameter space Θ, the system outputs $\boldsymbol{y}(\boldsymbol{u}, \boldsymbol{\theta_1}) = \boldsymbol{y}(\boldsymbol{u}, \boldsymbol{\theta_2})$ holds if and only if $\boldsymbol{\theta_1} = \boldsymbol{\theta_2}$.

Definition 3.2. Local identifiability: A system structure is said to be locally identifiable if for any parameter vector $\boldsymbol{\theta}$ within an open neighborhood of some point $\boldsymbol{\theta_*}$ in the parameter space Θ, the system outputs $\boldsymbol{y}(\boldsymbol{u}, \boldsymbol{\theta_1}) = \boldsymbol{y}(\boldsymbol{u}, \boldsymbol{\theta_2})$ holds if and only if $\boldsymbol{\theta_1} = \boldsymbol{\theta_2}$.

The key to the differential algebra method is the computation of the characteristic set. By deriving, substituting, and eliminating the unknown state variables, the final equation containing only the output variables and unknown parameters is called the input-output equation. Analyzing the coefficients of these equations reveals the identifiability of the parameter structure of the model [5]. The state variables we collecte from the literature are the concentrations of CD8$^+$ T cells T_k, CD4$^+$ T cells T_h, neutralizing antibodies A, memory CD8$^+$ T cells T_{km}, memory CD4$^+$ T cells T_{hm} and memory B cells B_m. Based on the clinical data, we analyze the structural identifiability of each of the above four models (see Table 1) by differ-

ential algebra. Here, we only show the analysis of **Model 3**. Since the three kinds of memory immune cells do not appear in the equations of the other variables, we can ignore them during our analysis, only using the data of T_k, T_h, A.

Theorem 3.1. *The structure of all parameters of* **Model 3** *is globally identifiable if the initial values of all variables and the clinical data T_k, T_h, A are known.*

Proof. For simplicity, we merge the corresponding humoral immunity and cellular immunity of **Model 3** into one model and express them in a simpler derivative notation, which yields the following system.

$$\begin{cases} I_1' = -\lambda I_1 T_k - \delta_I I_1, & t \neq \tau_i \quad (i = 1, 2, \ldots), \\ I_2' = \theta_1 S - \lambda I_2 T_k - \delta_I I_2, \\ S' = pI_1 - \beta SA - (\theta_1 + \theta_2) S, \\ T_k' = \omega_k T_k(\pi_k - T_k) + \alpha_k(I_1 + I_2), \\ T_h' = \omega_h T_h(\pi_h - T_h) + \alpha_h S, \\ B' = \omega_B B(\pi_B - B) + \alpha_B S T_h, \\ A' = \omega_A SB - \beta SA - \delta_A A. \end{cases} \tag{3.1}$$

First, we define the following partial ordering relation [5].

$$T_k < T_h < A < T_k' < T_k'' < \ldots < A < A' < \ldots <$$
$$I_1 < I_2 < S < B < I_1' < I_2' < \ldots < I_1'' < I_2'' < \ldots.$$

The largest one in an equation is the leader, and the equations are reordered according to their leaders from smallest to largest and shifted to the same side of the equations, resulting in

$$\begin{cases} T_k' - \omega_k T_k(\pi_k - T_k) - \alpha_k(I_1 + I_2) = 0, & \text{(leader: } I_2\text{)} \quad (3.2a) \\ T_h' - \omega_h T_h(\pi_h - T_h) - \alpha_h S = 0, & \text{(leader: } S\text{)} \quad (3.2b) \\ A' - \omega_A SB + \beta SA + \delta_A A = 0, & \text{(leader: } B\text{)} \quad (3.2c) \\ I_1' + \lambda I_1 T_k + \delta_I I_1 = 0, & \text{(leader: } I_1'\text{)} \quad (3.2d) \\ I_2' - \theta_1 S + \lambda I_2 T_k + \delta_I I_2 = 0, & \text{(leader: } I_2'\text{)} \quad (3.2e) \\ S' - pI_1 + \beta SA + (\theta_1 + \theta_2) S = 0, & \text{(leader: } S'\text{)} \quad (3.2f) \\ B' - \omega_B B(\pi_B - B) - \alpha_B S T_h = 0. & \text{(leader: } B'\text{)} \quad (3.2g) \end{cases}$$

Then, we calculate the input-output equations.

1. Since (3.2g) contains the leader B of (3.2c), from (3.2c) we get

$$\begin{aligned} B &= \frac{A' + \beta SA + \delta_A A}{\omega_A S}, \\ B' &= \frac{A'' + \beta S'A + \beta SA' + \delta_A A'}{\omega_A S} - \frac{(A' + \beta SA + \delta_A A) S'}{\omega_A S^2}. \end{aligned} \tag{3.3}$$

By substituting (3.3) into (3.2g) and simplifying it, we get

$$\begin{aligned}&\omega_A SA'' + \beta\omega_A S^2A' + \omega_A\delta_A SA' - \omega_A S'A' - \omega_A\delta_A S'A - \omega_A\omega_B\pi_B SA'\\&+\omega_B A'^2 + 2\beta\omega_B SAA' + 2\omega_B\delta_A AA' - \beta\omega_A\omega_B\pi_B S^2A + \beta^2\omega_B S^2A^2\\&+2\beta\omega_B\delta_A SA^2 - \omega_A\omega_B\pi_B\delta_A SA + \omega_B\delta_A^2A^2 - \alpha_B\omega_A^2S^3T_h = 0. \quad \text{(leader: } S')\end{aligned} \tag{3.4}$$

2. Since (3.2c), (3.2f), and (3.4) contain the leader S of (3.2b), from (3.2b) we get

$$\begin{aligned}S &= \frac{1}{\alpha_h}(\omega_h T_h^2 - \omega_h\pi_h T_h + T_h'),\\S' &= \frac{1}{\alpha_h}(2\omega_h T_h T_h' - \omega_h\pi_h T_h' + T_h'').\end{aligned} \tag{3.5}$$

By substituting (3.5) into (3.2c) and simplifying it, we get

$$\begin{aligned}&\alpha_h A' - \omega_A\omega_h T_h^2B + \omega_A\omega_h\pi_h T_hB - \omega_A T_h'B + \beta\omega_h T_h^2A - \beta\omega_h\pi_h T_hA\\&+\beta T_h'A + \alpha_h\delta_A A = 0. \quad \text{(leader: } B)\end{aligned} \tag{3.6}$$

By substituting (3.5) into (3.2f) and simplifying it, we get

$$\begin{aligned}&2\omega_h T_hT_h' - \omega_h\pi_h T_h' + T_h'' - p\alpha_h I_1 + \beta\omega_h T_h^2A - \beta\omega_h\pi_h T_hA + \beta T_h'A\\&+(\theta_1+\theta_2)\omega_h T_h^2 - (\theta_1+\theta_2)\omega_h\pi_h T_h + (\theta_1+\theta_2)T_h' = 0. \quad \text{(leader: } I_1)\end{aligned} \tag{3.7}$$

By substituting (3.5) into (3.4) and simplifying it, we get

$$\begin{aligned}&-\alpha_h\beta\omega_A\omega_B\omega_h^2\pi_B T_h^4A - \alpha_h^2\omega_A\omega_B\omega_h\pi_B\delta_A T_h^2A - 2\alpha_h\beta^2\omega_B\omega_h\pi_h T_hT_h'A^2\\&-2\alpha_h^2\beta\omega_B\omega_h\pi_h\delta_A T_hA^2 - 2\alpha_h^2\beta\omega_B\omega_h\pi_h T_hAA' + \alpha_h^2\omega_A\omega_B\omega_h\pi_B\pi_h T_hA'\\&-2\alpha_h\beta\omega_A\omega_h\pi_h T_hT_h'A' - \alpha_h^2\omega_A\omega_h\pi_h T_hA'' + 2\alpha_h\beta\omega_A\omega_B\omega_h^2\pi_B\pi_h T_h^3A\\&-\alpha_h\beta\omega_A\omega_B\omega_h^2\pi_B\pi_h^2T_h^2A - 2\alpha_h\beta\omega_A\omega_B\omega_h\pi_B T_h^2T_h'A - \alpha_h^2\omega_A T_h''A'\\&+2\alpha_h\beta\omega_A\omega_B\omega_h\pi_B\pi_h T_hT_h'A + \alpha_h^2\omega_A T_h'A'' + \alpha_h^2\omega_A\omega_B\omega_h\pi_B\pi_h\delta_A T_hA\\&-2\alpha_h\beta^2\omega_B\omega_h^2\pi_h T_h^3A^2 + \alpha_h\beta^2\omega_B\omega_h^2\pi_h^2T_h^2A^2 - 2\alpha_h\beta\omega_A\omega_h^2\pi_h T_h^3A'\\&+2\alpha_h\beta^2\omega_B\omega_h T_h^2T_h'A^2 + 2\alpha_h^2\beta\omega_B\omega_h\delta_A T_h^2A^2 + \alpha_h\beta\omega_A\omega_h^2\pi_h^2T_h^2A'\\&+2\alpha_h^2\beta\omega_B\omega_h T_h^2AA' - \alpha_h^2\omega_A\omega_B\omega_h\pi_B T_h^2A' + 2\alpha_h\beta\omega_A\omega_h T_h^2T_h'A'\\&-2\alpha_h^2\omega_A\omega_h\delta_A T_hT_h'A - \alpha_h^2\omega_A\omega_h\pi_h\delta_A T_hA' - \alpha_h\beta\omega_A\omega_B\pi_B T_h'^2A\\&-\alpha_h^2\omega_A\omega_B\pi_B\delta_A T_h'A + \alpha_h^2\omega_A\omega_h\pi_h\delta_A T_h'A + \alpha_h\beta^2\omega_B\omega_h^2T_h^4A^2\\&+6\alpha_B\omega_A^2\omega_h^2\pi_h T_h^4T_h' - 3\alpha_B\omega_A^2\omega_h^2\pi_h^2T_h^3T_h' + \alpha_h\beta\omega_A\omega_h^2T_h^4A'\\&+3\alpha_B\omega_A^2\omega_h\pi_h T_h^2T_h'^2 + \alpha_h^2\omega_A\omega_h\delta_A T_h^2A' + 2\alpha_h^2\beta\omega_B\delta_A T_h'A^2\\&-2\alpha_h^2\omega_A\omega_h T_hT_h'A' + 2\alpha_h^2\beta\omega_B T_h'AA' - \alpha_h^2\omega_A\omega_B\pi_B T_h'A' + \alpha_h^2\omega_A\omega_h\pi_h T_h'A'\\&+3\alpha_B\omega_A^2\omega_h^3\pi_h T_h^6 - 3\alpha_B\omega_A^2\omega_h^3\pi_h^2T_h^5 + \alpha_B\omega_A^2\omega_h^3\pi_h^3T_h^4 - 3\alpha_B\omega_A^2\omega_h^2T_h^5T_h'\end{aligned}$$

$$
\begin{aligned}
&- 3\alpha_B\omega_A^2\omega_h T_h^3 T_h'^2 + \alpha_h\beta^2\omega_B T_h'^2 A^2 + 2\alpha_h^3\omega_B\delta_A AA' + \beta\alpha_h\omega_A T_h'^2 A' \\
&+ \alpha_h^2\omega_A\delta_A T_h' A' + \alpha_h^3\omega_B A'^2 - \alpha_B\omega_A^2\omega_h^3 T_h^7 + \alpha_h^3\omega_B\delta_A^2 A^2 \\
&- \alpha_B\omega_A^2 T_h T_h'^3 + \alpha_h^2\omega_A\omega_h T_h^2 A'' - \alpha_h^2\omega_A\delta_A T_h'' A = 0. \qquad \text{(leader: } A'')
\end{aligned} \tag{3.8}
$$

3. Since (3.2e) contains the leader I_2 of (3.2a), from (3.2a) we get

$$
\begin{aligned}
I_2 &= \frac{1}{\alpha_k}(\omega_k T_k^2 - \omega_k\pi_k T_k + T_k' - \alpha_k I_1), \\
I_2' &= \frac{1}{\alpha_k}(2\omega_k T_k T_k' - \omega_k\pi_k T_k' + T_k'' - \alpha_k I_1').
\end{aligned} \tag{3.9}
$$

By substituting (3.9) into (3.2e) and simplifying it, we get

$$
\begin{aligned}
&2\omega_k T_k T_k' - \omega_k\pi_k T_k' + T_k'' - \alpha_k I_1' + (\lambda T_k + \delta_I)(\omega_k T_k^2 - \omega_k\pi_k T_k + T_k' - \alpha_k I_1) \\
&-\alpha_k\theta_1 S = 0. \qquad \text{(leader: } I_1')
\end{aligned} \tag{3.10}
$$

4. Since (3.2a), (3.2d), and (3.10) contain the leader I_1 of (3.7), from (3.7) we get

$$
\begin{aligned}
I_1 = \frac{1}{p\alpha_h}&[\beta\omega_h T_h^2 A - \beta\omega_h\pi_h T_h A + (\theta_1+\theta_2)\omega_h T_h^2 - (\theta_1+\theta_2)\omega_h\pi_h T_h \\
&+2\omega_h T_h T_h' + \beta T_h' A - \omega_h\pi_h T_h' + (\theta_1+\theta_2)T_h' + T_h''], \\
I_1' = \frac{1}{p\alpha_h}&[\beta\omega_h T_h^2 A' + 2\beta\omega_h T_h T_h' A - \beta\omega_h\pi_h T_h A' - \beta\omega_h\pi_h T_h' A \\
&+2(\theta_1+\theta_2)\omega_h T_h T_h' - (\theta_1+\theta_2)\omega_h\pi_h T_h' + 2\omega_h T_h'^2 + 2\omega_h T_h T_h'' \\
&+\beta T_h' A' + \beta T_h'' A - \omega_h\pi_h T_h'' + (\theta_1+\theta_2)T_h'' + T_h'''].
\end{aligned} \tag{3.11}
$$

By substituting (3.11) into (3.2a) and simplifying it, we get

$$
\begin{aligned}
&p\alpha_h T_k' - p\alpha_h\omega_k\pi_k T_k + p\alpha_h\omega_k T_k^2 - \alpha_k\beta\omega_h A T_h^2 + \alpha_k\beta\omega_h\pi_h T_h A \\
&-(\theta_1+\theta_2)\alpha_k\omega_h T_h^2 + (\theta_1+\theta_2)\alpha_k\omega_h\pi_h T_h - 2\alpha_k\omega_h T_h T_h' - \alpha_k\beta T_h' A \\
&+\alpha_k\omega_h\pi_h T_h' - (\theta_1+\theta_2)\alpha_k T_h' - \alpha_k T_h'' - p\alpha_k\alpha_h I_2 = 0. \qquad \text{(leader: } I_2)
\end{aligned} \tag{3.12}
$$

By substituting (3.11) into (3.2d) and simplifying it, we get

$$
\begin{aligned}
&\lambda\beta\omega_h T_k T_h^2 A - (\theta_1+\theta_2)\lambda\omega_h\pi_h T_k T_h - \beta\omega_h\pi_h\delta_I T_h A - \lambda\beta\omega_h\pi_h T_k T_h A \\
&+ T_h''' + 2\omega_h T_h T_h'' + \beta T_h'' A - \omega_h\pi_h T_h'' + \lambda T_k T_h'' + 2\omega_h T_h'^2 + \beta T_h' A' \\
&+ (\theta_1+\theta_2)T_h'' + \delta_I T_h'' + (\theta_1+\theta_2)\delta_I T_h' + 2\beta\omega_h T_h T_h' A - \beta\omega_h\pi_h T_h A' \\
&- \beta\omega_h\pi_h T_h' A + (\theta_1+\theta_2)\lambda T_k T_h' + (\theta_1+\theta_2)\omega_h\delta_I T_h^2 + 2\omega_h\delta_I T_h T_h' \\
&+ \beta\delta_I T_h' A - \omega_h\pi_h\delta_I T_h' + \lambda\beta T_k T_h' A - \lambda\omega_h\pi_h T_k T_h' + \beta\omega_h\delta_I T_h^2 A \\
&- (\theta_1+\theta_2)\omega_h\pi_h\delta_I T_h + (\theta_1+\theta_2)\lambda\omega_h T_k T_h^2 + 2\lambda\omega_h T_k T_h T_h'
\end{aligned}
$$

$$+\beta\omega_h T_h^2 A' + 2(\theta_1+\theta_2)\omega_h T_h T_h' - (\theta_1+\theta_2)\omega_h\pi_h T_h' = 0. \qquad \text{(leader: } A'\text{)} \tag{3.13}$$

By substituting (3.5) and (3.11) into (3.10) and simplifying it, we get

$$\begin{aligned}
&-2\alpha_k\beta\omega_h T_h T_h' A + \alpha_k\beta\omega_h\pi_h T_h A' + \alpha_k\beta\omega_h\pi_h T_h' A - (\theta_1+\theta_2)\lambda\alpha_k\omega_h T_k T_h^2\\
&-2\lambda\alpha_k\omega_h T_k T_h T_h' - \lambda\alpha_k\beta T_k T_h' A + \lambda\alpha_k\omega_h\pi_h T_k T_h' - \alpha_k\beta\omega_h\delta_I T_h^2 A\\
&+(\theta_1+\theta_2)\alpha_k\omega_h\pi_h\delta_I T_h + p\theta_1\alpha_k\omega_h\pi_h T_h - p\theta_1\alpha_k T_h' + \lambda\alpha_k\beta\omega_h\pi_h T_k T_h A\\
&-\lambda\alpha_k\beta\omega_h T_k T_h^2 A + (\theta_1+\theta_2)\lambda\alpha_k\omega_h\pi_h T_k T_h + \alpha_k\beta\omega_h\pi_h\delta_I T_h A\\
&+p\alpha_h\omega_k\delta_I T_k^2 - \alpha_k\beta T_h' A' - (\theta_1+\theta_2)\alpha_k\delta_I T_h' + 2p\alpha_h\omega_k T_k T_k' - p\alpha_h\omega_k\pi_k T_k'\\
&+p\lambda\alpha_h\omega_k T_k^3 + p\lambda\alpha_h T_k T_k' - \alpha_k T_h''' - 2\alpha_k\omega_h T_h T_h'' - \alpha_k\beta T_h'' A\\
&+\alpha_k\omega_h\pi_h T_h'' - \lambda\alpha_k T_k T_h'' - \alpha_k\delta_I T_h'' + p\alpha_h T_k'' - (\theta_1+\theta_2)\alpha_k T_h''\\
&+p\alpha_h\delta_I T_k' - 2\alpha_k\omega_h T_h'^2 - 2\alpha_k\omega_h\delta_I T_h T_h' - \alpha_k\beta\delta_I T_h' A + \alpha_k\omega_h\pi_h\delta_I T_h'\\
&-p\lambda\alpha_h\omega_k\pi_k T_k^2 - p\alpha_h\omega_k\pi_k\delta_I T_k - \alpha_k\beta\omega_h T_h^2 A' - 2(\theta_1+\theta_2)\alpha_k\omega_h T_h T_h'\\
&+(\theta_1+\theta_2)\alpha_k\omega_h\pi_h T_h' - (\theta_1+\theta_2)\lambda\alpha_k T_k T_h' - (\theta_1+\theta_2)\alpha_k\omega_h\delta_I T_h^2\\
&-p\theta_1\alpha_k\omega_h T_h^2 = 0. \qquad \text{(leader: } A'\text{)}
\end{aligned} \tag{3.14}$$

5. Since (3.14) contains the leader A' of (3.13), by (3.13) we get A', and substitute it into (3.14) and simplify it, we get

$$\begin{aligned}
&\lambda\alpha_h\omega_k T_k^3 - \lambda\alpha_h\pi_k\omega_k T_k^2 + \alpha_h\omega_k\delta_I T_k^2 - \alpha_h\omega_k\pi_k\delta_I T_k - \theta_1\alpha_k\omega_h T_h^2\\
&+\theta_1\alpha_k\omega_h\pi_h T_h + \lambda\alpha_h T_k T_k' + 2\alpha_h\omega_k T_k T_k' - \alpha_h\omega_k\pi_k T_k' + \alpha_h\delta_I T_k'\\
&-\theta_1\alpha_k T_h' + \alpha_h T_k'' = 0. \qquad \text{(leader: } T_h'\text{)}
\end{aligned} \tag{3.15}$$

6. Finally, the equations (3.15), (3.8), (3.13), (3.7), (3.12), (3.2b), (3.6) in order can not be further simplified. They form the characteristic set of (3.2), where the first three equations contain only the output variables T_k, T_h, A and their derivatives of each order, and thus form the input-output equations. Despite their complicated form, we only need to extract some coefficients for testing. Before that, to ensure good results, the three equations are normalized by eliminating the coefficient $\alpha_h^2\omega_A\omega_h$ of $T_h^2 A''$ in (3.8) and the coefficient α_h of T_k'' in (3.15). Since the coefficient of T_h''' in (3.13) is already 1, no further processing is needed.

Let another set of parameters $\boldsymbol{u} = (u_1, u_2, \ldots, u_{17})$ (corresponding to the parameters in Table 5 in order) satisfy the input-output equations. Extracting the coefficients of $T_h'' A, T_h T_h^3, T_h^4 A, T_h''^2 A^2$ from (3.8), the coefficients of $T_h T_h'', T_h'' A, T_k T_h'', T_h A', T_h^2 A, T_h^2$ from (3.13), and the coefficients of $T_k^3, T_k^2, T_k', T_h^2$ from (3.15), we get

the following equations

$$\begin{cases} -\dfrac{\delta_A}{\omega_h} = -\dfrac{u_{10}}{u_{13}}, \\ -\dfrac{\alpha_B\omega_A}{\alpha_h\omega_h} = -\dfrac{u_8u_{11}}{u_7u_{13}}, \\ \dfrac{\beta\omega_B\omega_h\pi_B}{\alpha_h} = \dfrac{u_3u_{14}u_{13}u_{17}}{u_7}, \\ 2\omega_h = 2u_{13}, \\ \beta = u_3, \\ \lambda = u_2, \\ -\beta\omega_h\pi_h = -u_3u_{13}u_{16}, \end{cases} \quad \text{and} \quad \begin{cases} \beta\omega_h\delta_I = u_3u_{13}u_9, \\ (\theta_1+\theta_2)\omega_h\delta_I = (u_4+u_5)u_{13}u_9, \\ \lambda\omega_k = u_2u_{12}, \\ \omega_k(\delta_I - \lambda\pi_k) = u_{12}(u_9 - u_2u_{15}), \\ \alpha_h(\delta_I - \omega_k\pi_k) = u_7(u_9 - u_{12}u_{15}), \\ -\dfrac{\theta_1\alpha_k}{\alpha_h} = -\dfrac{u_4u_6}{u_7}, \\ \dfrac{\beta^2\omega_B}{\alpha_h\omega_A\omega_h} = \dfrac{u_3^2u_{14}}{u_7u_{11}u_{13}}. \end{cases}$$

By solving them, we get

$$\begin{cases} \delta_A = u_{10}, \\ \alpha_B\omega_A = u_8u_{11}, \\ \omega_B\pi_B = u_{14}u_{17}, \\ \omega_h = u_{13}, \\ \beta = u_3, \\ \lambda = u_2, \\ \pi_h = u_{16}, \end{cases} \quad \text{and} \quad \begin{cases} \delta_I = u_9, \\ \theta_1+\theta_2 = u_4+u_5, \\ \omega_k = u_{12}, \\ \pi_k = u_{15}, \\ \alpha_h = u_7, \\ \theta_1\alpha_k = u_4u_6, \\ \dfrac{\omega_B}{\omega_A} = \dfrac{u_{14}}{u_{11}}. \end{cases} \tag{3.16}$$

In addition, we find that even if we use the coefficients of the other terms in the equations, we cannot get a better result. Therefore, if only the clinical data T_k, T_h, A are known, the parameters $p, \theta_1, \theta_2, \alpha_k, \alpha_B, \omega_A, \omega_B, \pi_B$ are unidentifiable, while the structure of the rest parameters is globally identifiable.

Considering that the initial values of each variable in the model are known, the remaining four equations of the characteristic set at $t = t_0$ can be considered input-output equations as well. Extracting the coefficient of T_h^2B from (3.6), the coefficient of I_1 from (3.7), and the coefficient of T_h'' from (3.12), the following equations are obtained:

$$\begin{cases} -\omega_A\omega_h = -u_{11}u_{13}, \\ p\alpha_h = u_1u_7, \\ -\alpha_k = -u_6. \end{cases}$$

Meanwhile, considering (3.16), we get

$$\begin{cases} \omega_A = u_{11}, \\ \alpha_B = u_8, \\ \omega_B = u_{14}, \\ \pi_B = u_{17}, \end{cases} \quad \text{and} \quad \begin{cases} p = u_1, \\ \alpha_k = u_6, \\ \theta_1 = u_4, \\ \theta_2 = u_5. \end{cases}$$

Thus the structure of the system (3.1) is globally identifiable, i.e., the changes of the variables are completely known if the initial values are known.

In summary, in the case where the initial values of all variables are known and the variables T_k, T_h, A are output variables, there is only one unique set of parameters that can satisfy the output variables, hence, the structure of **Model 3** is globally identifiable. □

Similarly, we can obtain the structural identifiability of **Model 1**, **Model 2** and **Model 4**. Due to the complicated calculations, we only give the results of structural identifiability for the other three models, and we will not repeat the details of the proof.

Theorem 3.2. *The structures of* **Model 1** *and* **Model 2** *are unidentifiable if the initial values of all variables and the clinical data $T_k, T_h, A, T_{km}, T_{hm}, B_m$ are known. But as long as any one of the parameters $\alpha_B, \pi_B, \omega_B, \omega_A, \gamma_B, \mu_B$ is known, the structures of* **Model 1** *and* **Model 2** *are globally identifiable.*

Meanwhile, from Theorem 3.1 we can directly obtain the corresponding conclusion of **Model 4**.

Theorem 3.3. *The structure of all parameters of* **Model 4** *is globally identifiable if the initial values of all variables and the clinical data T_k, T_h, A are known.*

Whether the model is reasonable or not, and whether the prediction results are robust or not, are closely related to the reliability of the parameter estimation. The credibility of parameter estimation depends on whether the structure of the model is identifiable or not. Therefore, we first analyze the structural identifiability of the models before further research. In this section, we show that two of the four models are globally identifiable under the available clinical data (**Model 3** and **Model 4**) while the other two are unidentifiable (**Model 1** and **Model 2**). This provides theoretical support for the following parameter estimation and model selection.

4. Data fitting and model selection

We often want to use a simple model to describe the viral infection process, but we are concerned that simplicity may overlook some important factors, which requires the modelers to select among the models with different complexities. It is worthwhile to investigate how to select a model that best represents the dynamic responses of the vaccines or the viruses in the hosts from a large number of models with limited clinical data.

Japanese researcher Hirotugu Akaike proposed a model selection method in 1973: Akaike's Information Criterion (AIC). He pointed out that when trying to select an optimal model from a set of candidate models, the one with the smallest AIC

value [1–3] should be chosen. Common model selection criteria are AIC and BIC, given the large numbers of parameters, we use the corrected AIC, i.e. AICc, for model selection, which is calculated by the following formula [35]

$$AICc = -2\ln(L(\hat{\theta}_{MLE})) + 2K + \frac{2K(K+1)}{N-K-1}, \tag{4.1}$$

where, K is the number of unknown parameters, N is the number of observations, and L is the likelihood function. The smaller the value of AICc, the better the model.

We are going to use the Affine Invariant Ensemble Markov Chain Monte Carlo (GWMCMC) algorithm [14] for parameter estimation. The traditional Markov Chain Monte Carlo algorithm approximates the posterior distribution of the parameters by randomly sampling the parameter space [12]. The GWMCMC algorithm we use is superior to the Metropolis-Hastings (M-H) algorithm and the Random Walk M-H algorithm [7], especially when the parameters are unidentifiable. The advantage of this algorithm is that it does not take into account the normalization of the parameters and is iterated by several walkers at the same time. The positions of the walkers are based on the current positions of all other walkers, which makes the estimation more accurate. Details of the algorithm can be found in the literature [14, 34]. In this study, we assume that all known data have normally distributed noise. The meanings, prior ranges, and sources of the parameters in the paper are given in Table 5.

Also, the MCMC algorithm needs to be determined whether it has converged or not. This crucial aspect is often avoided. If the Markov Chain has not yet reached the convergence state, it means that the result has not yet reached the target posterior distribution, and further iterations are needed to get a better result. The existing convergence theorem can only theoretically guarantee that it will converge to the target distribution [19] after a sufficiently long iteration, but it cannot tell us quantitatively how long it will take. In general, we can judge whether it has converged subjectively by drawing an iterative graph. In addition to this observation method, we can also use the method proposed by Gelman et al. [6,10], which utilizes the idea of analysis of variance (ANOVA) to construct an estimator $\hat{V}$ of the variance σ^2 and compute the potential scale reduction factor (PSRF) to determine whether it has converged.

It can be considered that the chain has converged when PSRF ≈ 1, otherwise it is necessary to continue iterating or to look for other ways to help it converge.

Based on the above GWMCMC algorithm and convergence criteria, we first select the optimal one among four models (see Table 1) using the clinical data of Moderna's vaccine mRNA-1273 and find a set of optimal parameter posterior distributions, optimal values, and their 95% confidence intervals for each model.

We performed about 100 million iterations on 34 chains, with 3 million steps per chain. Since the iterations of each chain are performed simultaneously, the iteration steps mentioned below are for a single chain. We save the results every 10 iterations and calculate the PSRF values of each parameter for $10\times 2^n (n = 1, \ldots, 17)$ iterations. In addition, because the result at the beginning of iteration is unstable, to eliminate its side effect, when the number of iteration steps is more than 400 thousand steps, only the result of the first 400 thousand steps of the current step number is taken for calculation. Here we only show the result based on the mRNA-1273 (Figure 2), and it is easy to see that PSRFs are approaching 1.

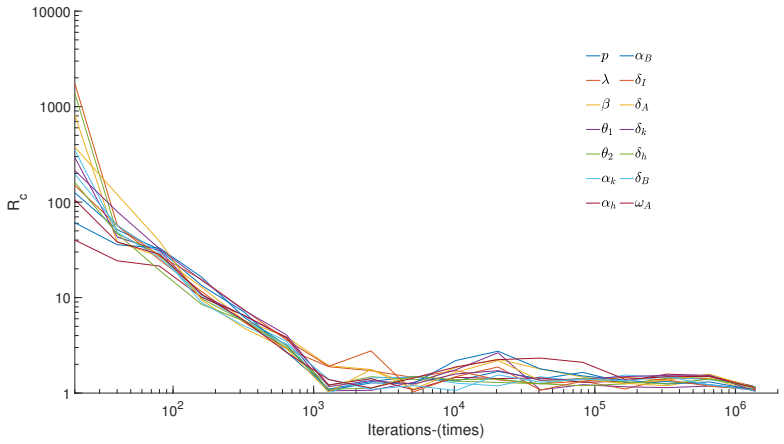

Figure 2. Convergence of PSRF. Every line shows the PSRF of one specific parameter converging to 1 with transitions when we fit the data of mRNA-1273.

The parameter estimation results of the four models are shown in Table 2 with respect to mRNA-1273. For model selection, we calculate the corresponding AICc values by using the formula (4.1) and corroborate them with the BIC values, and the results are shown in Table 3. Obviously, correlation values of **Model 3** are the smallest among the four models, whether the AICc value or the BIC value is used as the criterion for model selection. This suggests that **Model 3** is the most suitable of the four models for describing the dynamics of mRNA vaccination and the clinical data collected. In addition, this result also suggests that the killing of infected cells by memory cells and the promotion of immune cells and neutralizing antibodies by memory cells during mRNA vaccination are not significant and can be ignored. On the other hand, the fact that **Model 4** is not selected implies that the role of the body's inherent innate immunity in this process cannot be ignored. The blue curves in Figure 3 are the fitting results of the selected model **Model 3** under the optimal parameters, and the upper arrows represent the time points of vaccination. Finally, we perform the same process on the data of the mRNA vaccine BNT162b2 from Pfizer/BioNTech and obtain results consistent with the vaccine mRNA-1273. The fitting results of the selected model **Model 3** are shown by the brown curves in Figure 3. The fitting results show that both vaccines can significantly increase the numbers of immune cells and neutralizing antibodies, among which the increase of $CD8^+$ T cells, $CD4^+$ T cells, and neutralizing antibodies are more obvious and remain at high levels on day 181. This suggests that the vaccine can enhance the immunity against SARS-CoV-2.

Also can be seen from Figure 3, different variables peak at different time points. After the first vaccination of mRNA-1273, $CD8^+$ T cells, $CD4^+$ T cells, and neutralizing antibodies respectively peak on day 21, day 19, and day 26, which shows that the components of the immunity system are decreasing on day 27, the day one gets the second vaccination. So, this may mean one can be vaccinated a little earlier. By contrast, the day one is vaccinated with the second BNT162b2 is generally the day the effect of vaccination peaks. The time points of the two vaccinations are better articulated than mRNA-1273.

Table 2. mRNA-1273 Optimal Value and 95% CI.

Parameter	Model 1		Model 2		Model 3		Model 4	
	Optimal Value	95% CI	Optimal Value	95% CI	Optimal Value	95% CI	Optimal Value	95% CI
p	211	(201, 230)	197	(190, 230)	200	(196, 230)	210	(207, 217)
λ	0.086	(0.083, 0.11)	0.085	(0.083, 0.12)	0.1	(0.09, 0.12)	0.12	(0.11, 0.12)
β	9.9e-14	(8e-14, 1.2e-13)	1.05e-13	(8.6e-14, 1.2e-13)	1e-13	(8e-14, 1.17e-13)	1.1e-13	(1e-13, 1.1e-13)
θ_1	0.037	(0.03, 0.041)	0.045	(0.03, 0.045)	0.038	(0.03, 0.044)	0.03	(0.03, 0.032)
θ_2	0.19	(0.16, 0.21)	/	/	0.17	(0.15, 0.21)	/	/
α_k	8.5e-7	(7.3e-7, 1e-6)	9.8e-7	(8.3e-7, 1e-6)	8.5e-7	(7.6e-7, 1e-6)	8.3e-7	(8.1e-7, 8.7e-7)
α_h	3.14e-6	(2.54e-6, 3.48e-6)	2.9e-6	(2.4e-6, 3.4e-6)	3e-6	(2.4e-6, 3.6e-6)	3.4e-6	(3.2e-6, 3.5e-6)
α_B	2.25e-6	(2.02e-6, 2.92e-6)	2.8e-6	(2e-6, 3e-6)	2.5e-6	(2e-6, 3e-6)	2.7e-6	(2.6e-6, 2.9e-6)
δ_I	0.012	(0.011, 0.012)	0.012	(0.009, 0.012)	0.01	(0.008, 0.012)	0.012	(0.012, 0.0124)
δ_A	0.031	(0.028, 0.042)	0.021	(0.018, 0.03)	0.031	(0.026, 0.035)	0.039	(0.038, 0.05)
ω_A	596	(547, 626)	501	(484, 540)	563	(521, 591)	619	(572, 712)
ω_k	0.32	(0.29, 0.39)	0.3	(0.26, 0.4)	0.33	(0.26, 0.33)	0.35	(0.33, 0.37)
ω_h	0.011	(0.011, 0.013)	0.01	(0.009, 0.012)	0.011	(0.009, 0.013)	0.013	(0.012, 0.013)
ω_B	0.078	(0.075, 0.079)	0.113	(0.104, 0.116)	0.1	(0.096, 0.114)	0.089	(0.086, 0.094)
γ_k	0.008	(0.007, 0.011)	0.008	(0.007, 0.01)	/	/	/	/
γ_h	0.0014	(0.0014, 0.002)	0.0015	(0.0014, 0.002)	/	/	/	/
γ_B	6e-6	(5.7e-6, 6e-6)	5.8e-6	(4.6e-6, 6e-6)	/	/	/	/
η_k	4.6e-6	(4e-6, 5.3e-6)	4.8e-6	(4.2e-6, 5.2e-6)	/	/	/	/
η_h	1.42e-7	(1.12e-7, 1.68e-7)	1.5e-7	(1.1e-7, 1.7e-7)	/	/	/	/
η_B	1.3e-7	(1.2e-7, 1.6e-7)	1.7e-7	(1.2e-7, 1.8e-7)	/	/	/	/
δ_k	0.56	(0.52, 0.64)	0.62	(0.58, 0.66)	/	/	/	/
δ_h	0.024	(0.018, 0.024)	0.016	(0.016, 0.021)	/	/	/	/
δ_B	4.8e-4	(4.1e-4, 4.8e-4)	3.7e-4	(3.2e-4, 4.5e-4)	/	/	/	/
μ_k	117	(100, 230)	134	(101, 356)	/	/	/	/
μ_h	1310	(511, 2000)	100	(100, 365)	/	/	/	/
μ_B	992	(558, 1985)	294	(100, 1265)	/	/	/	/

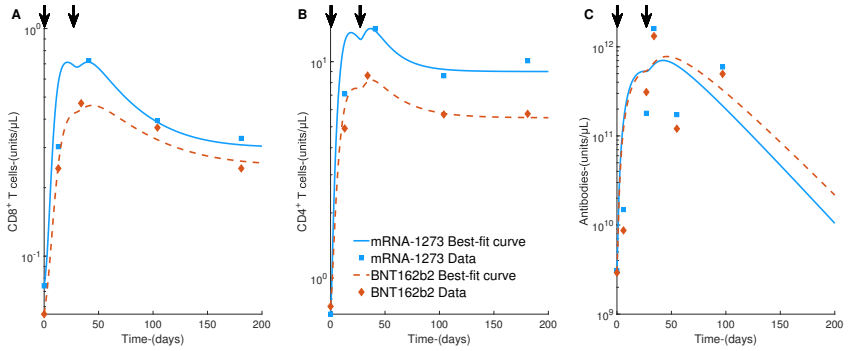

Figure 3. Fitting Results with GWMCMC of **Model 3**. The first vaccination is injected on day 0 and the second vaccination is injected on day 27. The blue lines and the brown dashed lines show the fitting results of the data of mRNA-1273 and BNT162b2 respectively. Squares and diamonds represent the processed data of two vaccines. The arrows mark the time points one is injected.

Table 3. List of AICc and BIC for Different Sub-models of mRNA-1273.

Model	Number of Parameters	AICc	BIC	Maximum Likelihood
Model 1	26	376.73	418.04	2.86e-84
Model 2	25	377.82	417.88	1.63e-84
Model 3	14	263.73	277.74	6.27e-59
Model 4	13	318.00	331.35	1.01e-70

5. Practical identifiability analysis

The structural identifiability discussed above is based on the premise that the data are free of noise. In reality, data are inevitably subject to measurement and processing errors, which leads to the question of practical identifiability, i.e., the effect of noise on fitting and estimation. A model whose structure is identifiable may not be practically identifiable [36]. Therefore, we simulate by exerting different levels of noise on the data to investigate the effect of noise on the system. We assume that the data have two types of noise: Gaussian error with standard deviations of 10% and 20%, respectively. We take the optimal parameters obtained by GWMCMC as the real values, add 1000 sets of random errors to the dynamics curves of variables T_k, T_h, A as the error dataset, and then fit them with GWMCMC again to obtain the optimal parameters with the noisy data. By calculating the average relative error (ARE) between these 1000 sets of optimal parameters and the true values, we present the results in Table 4.

ARE values can be used to quantitatively determine whether each parameter is practically identifiable or not. Obviously, for a practically identifiable parameter, the ARE value should be close to 0, and as the error increases, the ARE value increases. If the ARE of a parameter is large for a small error, it means that the error in the data causes the parameter estimate to be unreliable, i.e., the parameter is sensitive to changes in the data, and then the parameter is practically unidentifiable. However, although the ARE value can be used to analyze the practical identifiability, there is no universal standard, so different standards will lead to different results. Here, we refer to the method in [36], considering a parameter to be practically

Table 4. List of AREs of Parameters for **Model 3** with Measurement Error Levels 10% and 20%. *ARE > noise.

Parameter	True Value	$N(0, 10\%)$	$N(0, 20\%)$	Parameter	True Value	$N(0, 10\%)$	$N(0, 20\%)$
p	0.02	0.07	0.16	α_B	0.04	0.08	0.24*
λ	0.03	0.08	0.17	δ_I	0.03	0.07	0.14
β	0.04	0.15*	0.22*	δ_A	0.04	0.05	0.05
θ_1	0.02	0.14*	0.25*	ω_A	0.04	0.18*	0.27*
θ_2	0.02	0.10	0.15	ω_k	0.02	0.08	0.17
α_k	0.01	0.07	0.16	ω_h	0.03	0.09	0.17
α_h	0.03	0.06	0.09	ω_B	0.01	0.10	0.15

identifiable when the ARE value is not larger than the noise error of our simulation, and vice versa, it is considered practically unidentifiable.

In addition to the two errors we mentioned, we also simulated the noise-free case (assuming the noise is 0 and repeating the previous fitting procedure). As can be seen from Table 4, for the true values, the maximum ARE value for each parameter is 0.04. Considering the small number of iterations here (1 million steps), we consider this to be low enough, which suggests that the parameters can be uniquely determined for the noise-free data, which confirms that **Model 3** is globally identifiable. In addition, we find that the parameter α_B is practically identifiable at 10% noise, but becomes unidentifiable when the noise increases to 20%. Unfortunately, the parameters $\beta, \theta_1, \omega_A$ are practically unidentifiable at both noise levels. The remaining parameters are practically identifiable at both noise levels. To investigate how much these practically unidentifiable parameters affect the fit, we perform the following numerical simulation. The practically identifiable parameters are fixed to the optimal values fitted by **Model 3** (see Table 2), and the four unidentifiable parameters $\alpha_B, \beta, \theta_1, \omega_A$ are added with 10% and 20% standard deviations of normal distribution noise. We randomly sample parameters 10 thousand times each, and then we obtain the dynamics curves and their 95% confidence intervals of each variable in **Model 3**, which are shown in Figure 4. As can be seen from the figure, most of the variables maintain a narrow range under these 10 thousand samples, and only two variables, infected cells II and antibodies, have a wider range of confidence intervals, which are within acceptable limits. This indicates that our fitting results are generally reliable.

6. Parameter sensitivity analysis and virtual experiments

6.1. Parameter sensitivity analysis

In the previous section, we find that some of the parameters are practically unidentifiable. This suggests that errors in observations can lead to increased errors in parameter estimation, making the fit less robust. Conversely, the question of how much a change in a parameter may affect the predicted outcome is the parameter sensitivity analysis. This helps us to find the key parameters in the model that have a greater impact on the results, and through this process we can see which biological factors play a more important role in vaccination and the human immune

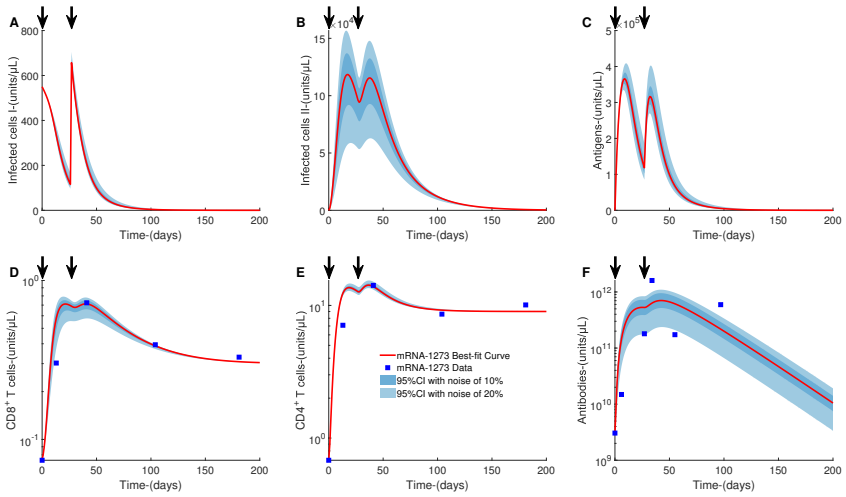

Figure 4. Effects of Practically Unidentifiable Parameters on the System. The red lines show the fitting results of the data of mRNA-1273. Squares represent the processed data. The shades are the 95% CIs with some parameters exerted noise of 10% and 20%. The arrows mark the time points one is injected.

response. In general, we can fix other factors and change a single factor, which is called local sensitivity analysis, but in biological processes, the factors are usually very uncertain, and they may be related to each other. Therefore, we use global sensitivity analysis [23] to study the sensitivity of models to the parameters more comprehensively.

We use Latin Hypercube Sampling (LHS) [26] to sample the parameters, and Partial Rank Correlation Coefficient (PRCC) values to perform the sensitivity analysis, to find out the parameters that most affect the model. The results of the sensitivity analysis are shown in Figure 5. It can be seen that the three important immune variables, $CD8^+$ T cells T_k, $CD4^+$ T cells T_h and antibodies A are insensitive to the parameters $p, \alpha_B, \delta_A, \omega_B$, whereas they are sensitive to the parameters $\lambda, \theta_1, \theta_2, \alpha_k, \omega_k$. These parameters are mostly related to $CD8^+$ T cells and antigens, so we can start from these two aspects to resist the viral infection process. In addition, we find that the parameters α_h, ω_h associated with $CD4^+$ T cells only have a significant effect on neutralizing antibodies, suggesting that although the $CD4^+$ T cells may not change much after vaccination, it is enough to effectively impact on the production of neutralizing antibodies.

6.2. Injection of the booster

One advantage of the mathematical model is that the experiments can be carried on easily with little cost. The effects of different strategies for epidemics can be compared directly [16,38]. For the real vaccinations with the mRNA vaccines against SARS-CoV-2, the first vaccination is usually injected on day 0, followed by a second vaccination on day 27. The body then produces a great quantity of antibodies that last for a long period. Subsequent vaccinations are often called "boosters" and are often given at intervals of no less than 6 months.

Next, we simulate the viral and immune dynamics in vivo after the initial two

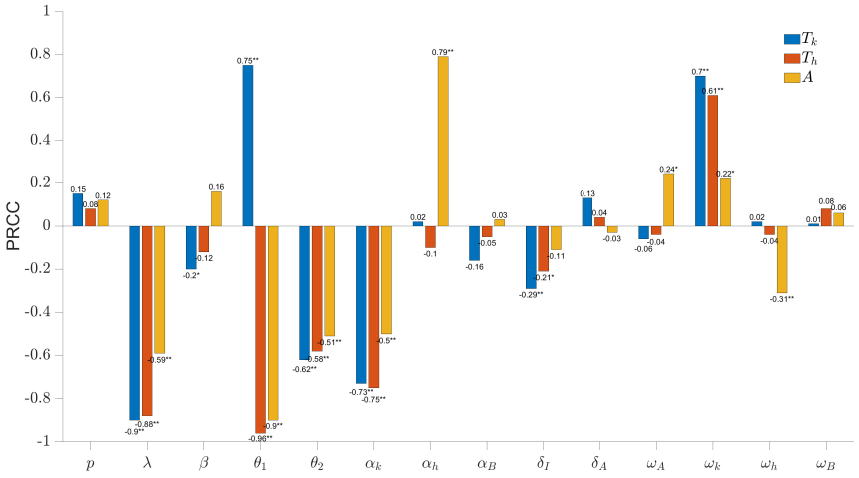

Figure 5. Sensitivity Analysis. PRCCs for T_k, T_h, A with all parameters. LHS is done 1 thousand times. $^{*}p < 0.05, ^{**}p < 0.01$.

vaccinations followed by booster injections at 6-month and 12-month intervals. Figure 6 is a numerical simulation based on the fitting results of Table 2 and **Model 3** (Results of BNT162b2 are shown in Appendix C). The arrows above the subfigures mark the time points one is injected. We find that after a period after the first two vaccinations, the immune cells $CD8^+$ T cells (Subfigure D) and $CD4^+$ T cells (Subfigure E) reach certain stable states with time, whereas the neutralizing antibodies (Subfigure F) show a continuous decline, and if the individual does not receive new vaccinations, the level of antibodies eventually drops to 0 after about 1 thousand days. Obviously, this simulation result is consistent with the theoretical result in Theorem 2.1. However, once the individual receives a booster injection 6 months later, all infected cells (Subfigure A, B), antigens (Subfigure C), immune cells (Subfigure D, E), and neutralizing antibodies (Subfigure F) increase rapidly to a peak a little lower than that of the second vaccination and then show a decreasing trend. Infected cells and antigens decrease the fastest, immune cells the second fastest, and neutralizing antibodies the slowest. The dynamics of the system are similar when an individual is vaccinated again after 12 months. However, according to Theorem 2.1, if an individual does not receive a new vaccination, the antibody level will eventually drop to 0 after a certain period. Therefore, boosters do maintain high levels of neutralizing antibodies for some time. Compared to neutralizing antibodies, boosters do not stimulate other immune cells as much. There are two hypotheses: one is that the immune system has already memorized the S proteins from the vaccine, so when the S proteins reappear in vivo, they will be bound by the rapidly produced antibodies; the other is that the antibody level is already relatively high, and the antibodies produced previously can bind to the S proteins. Both suggest that the antibodies are effective in stopping the viruses from proliferating and also further support the previous results of the parameter sensitivity analysis. In conclusion, we believe that the boosters can effectively enhance the resistance of the human body to viruses.

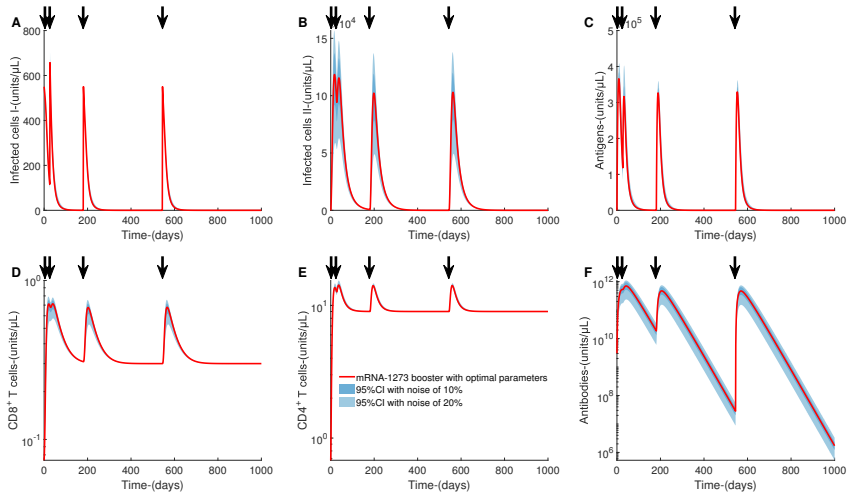

Figure 6. Injection of the Booster. The red lines show the dynamics after the boosters of mRNA-1273. The shades are the 95% CIs with some parameters exerted noise of 10% and 20%. The arrows mark the time points one is injected.

7. Discussion

Mathematical models are an effective means of analyzing biological processes. This paper investigates the microdynamics of the mRNA vaccine in vivo. We first develop a model describing the dynamics of infection in vivo after vaccination based on the characteristics of mRNA vaccines. Unfortunately, models of vaccines are rarely studied, and there is little literature to draw on. We propose four sub-models based on biological meanings and use the GWMCMC for data fitting and parameter estimation. Although the parameter space is very large, the parallel computation of the GWMCMC can help the iterations converge quickly. We obtain the optimal parameters and their 95% confidence intervals and calculate their AICc and BIC, which show that **Model 3** is the best under both criteria, i.e., the roles of memory cells can be ignored temporarily in the immunization induced by the first two vaccinations, and the innate immune mechanism cannot be ignored. We also calculate the PSRF to determine the convergence, and the results show that the Markov Chain can be considered to have reached convergence.

Assuming that the observed data are free of noise, the predictions of the structurally unidentifiable and locally identifiable cases may differ significantly, even though models with different parameter combinations can fit the observations well. To make the results more robust, structural identifiability analysis of the proposed system is critical, but it is neglected in many immunological modeling processes. We analyze the identifiability of the system using differential algebra. Based on immunological clinical data, we show that all four systems are either globally identifiable or if only one parameter needs to be known, the rest of the parameters are globally identifiable. This theoretically supports the reliability of parameter estimation by GWMCMC. The GWMCMC is a global optimization method that searches through the parameter space to obtain the posterior distribution of the parameters to maximize the fit to the data. Then we take these fitting results as

the basis for model selection for the four systems and find that **Model 3** is the best model among them for the collected clinical data, i.e., this model is the most suitable for explaining the interaction process between mRNA vaccines and the immune system. This suggests that the roles of memory cells in killing infected cells and promoting immune cells and neutralizing antibodies during mRNA vaccination are not significant and can be ignored in the modeling process. On the other hand, the fact that **Model 4** is not selected suggests that the innate immunity of the human body plays a necessary role in this process. We first analyze the optimal model theoretically, calculate the equilibria, and show that the disease-free equilibrium E_1 is globally asymptotically stable, while the boundary equilibria are unstable. This indicates that after vaccination, infected cells and antigens are no longer alive, and they are all killed due to the immune system or apoptosis. This supports the theoretical safety of mRNA vaccines.

Mathematical models play an important role in medical research. Of course, any nonlinear dynamic model cannot take into account all factors and is only an approximate representation of the actual situation. A good dynamic model can better describe the basic laws of the research objects. In addition, due to the complexity of the immune system, experimental immunologists often hold different views and interpretations on some of the phenomena, in which case theoretical analysis can help to determine which view or interpretation is more plausible and to know which factors play a major role. Sometimes the analysis and computation of theoretical models can lead to interesting results, which may predict a discovery. It is of course the most desirable. Even if this is not the case, it can be used as a reference for medical scientists to plan their experiments. Whether the result is positive or negative, we consider it valuable.

Appendix A. Model of the mRNA vaccine

The biological meanings of the variables in the system (2.1) and the system (2.2) are described as follows:

1. The equation for the variable S describes the dynamics of the antigens. When a vaccine is injected, it can only be produced by I_1 (the first term on the right side of the equation). Some of these antigens are neutralized by the neutralizing antibodies A that substitute for ACE2 receptors on the surface of the target cells (the second term), some are killed by the innate immune system [8], such as phagocytosis by macrophages, etc. ($\theta_2 S$ in the third term), the rest may infect healthy cells ($\theta_1 S$).
2. The equation for the variable I_1 describes the dynamics of the target cells entered by the mRNAs of the S proteins in the vaccine. We characterize the injection process of a multi-shot vaccine in the form of an impulsive differential equation. This type of infected target cells produce the antigens S. The first term on the right-hand side of the equation describes the killing of I_1 by immune cells, the $CD8^+$ T cells T_k and the memory $CD8^+$ T cells T_{km}, while the second term describes the natural apoptosis of these target cells.
3. The equation for the variable I_2 describes the dynamics of the target cells infected by the antigens. We assume that healthy target cells are infected by the antigens S produced by I_1. The intact viruses utilize the S proteins on

their surfaces to bind to the ACE2 receptors on the surfaces of the target cells, thereby opening the target cells and injecting the mRNAs of the intact viruses to replicate the viruses [11]. Therefore, as long as the immune system can deal with the S proteins, for example, by producing neutralizing antibodies that bind to these S proteins instead of ACE2 receptors, we can prevent the viruses from reproducing in vivo. So in an mRNA vaccine, the S proteins are the antigens. Since the mRNAs in an mRNA vaccine are only the mRNAs of the S proteins and not the mRNAs of the complete viruses, target cells infected with the S proteins will only stimulate the immune system but will not be able to produce complete viral particles. The first term on the right side of the equation describes the infection of healthy target cells by the antigens S, and the second term characterizes the killing of infected target cells by the $CD8^+$ T cells T_k and the memory $CD8^+$ T cells T_{km}, and the third term represents the natural apoptosis of infected target cells.

4. The equations for the variables T_k, T_h and B describe the dynamics of the $CD8^+$ T cells, the $CD4^+$ T cells and the B lymphocytes, respectively. The first term of each equation describes the growth of the immune component, while the second term characterizes the stimulation of the proliferation of each component by the infected target cells (I_1 and I_2), the antigens S, and the $CD4^+$ T cells, respectively.
5. The equation for the variable A describes the dynamics of neutralizing antibodies. The first term describes the interaction of the lymphocytes B and the memory lymphocytes B_m with the antigens S stimulating the production of more neutralizing antibodies A. The second term describes the consumption of neutralizing antibodies as a result of binding to the antigens S, and the third term represents the natural apoptosis of neutralizing antibodies.
6. The equations for the variables T_{km}, T_{hm} and B_m represent the memory $CD8^+$ T cells, the memory $CD4^+$ T cells and the memory B cells respectively. The first term of each equation describes the eventual transformation of a fraction of lymphocytes into the corresponding memory lymphocytes, the second term represents the rapid proliferation of the corresponding memory cells when stimulated by infected target cells or antigens, and the third term represents the natural apoptosis of the memory cells.

Here we have ignored other details and intermediate processes, such as the involvement of plasma cells, antigen-presenting cells, etc. [17, 30]. For the sake of practicality, it is also assumed that the vaccine is injected in a pulsatile manner. To do this, we need to add the following conditions:

$$I_1(\tau_i^+) = I_1(\tau_i) + I_{1i}, \qquad t = \tau_i \qquad (i = 1, 2, \ldots).$$

This equation represents the increase of I_1 due to the injection of a new vaccine at the moment of τ_i $(i = 1, 2, \ldots)$, where $I_1(\tau_i)$ denotes the number of target cells infected in the original system at the moment of τ_i, and I_{1i} denotes the number of target cells newly infected by the mRNAs of the S proteins in the newly injected vaccine. The meanings of the parameters in the system (2.1) & (2.2) are summarized in Table 5.

Considering the equilibria of the dynamic model of the vaccine in vivo. Letting both (2.1) and (2.2) be $\mathbf{0}$, it is easy to know that there are 8 equilibria as follows:

$\boldsymbol{E_1}(I_1, I_2, S, T_k, T_h, B, A, T_{km}, T_{hm}, B_m)$

Table 5. Parameters of the System (2.1) & (2.2).

Parameter	Biological Meaning	Prior Ranges/Values	Source
p	Proliferation rate of antigens	$[1.9e2,\ 2.3e2]$	Estimated
λ	Killing rate of $CD8^+$ T cells against infected cells	$[7e-2,\ 1.5e-1]$	Estimated
β	Binding rate of antibodies and antigens	$[7e-14,\ 1.5e-13]$	Estimated
θ_1	Infection rate of cells by antigens	$[2e-2,\ 6e-1]$	Estimated
θ_2	Killing rate of innate immunity against antigens	$[1.5e-1,\ 6e-1]$	Estimated
α_k	Stimulation of $CD8^+$ T cells by infected cells	$[4e-7,\ 1.2e-6]$	Estimated
α_h	Stimulation of $CD4^+$ T cells by antigens	$[2e-6,\ 5e-6]$	Estimated
α_B	Stimulation of B cells by antigens and $CD4^+$ T cells	$[8e-8,\ 3.5e-6]$	Estimated
δ_I	Apoptosis rate of infected cells	$[8e-3,\ 1.4e-2]$	Estimated
δ_A	Apoptosis rate of neutralizing antibodies	$[8e-3,\ 1e-1]$	Estimated
ω_A	Growth rate of neutralizing antibodies	$[2e2,\ 3e3]$	Estimated
ω_k	Growth rate of $CD8^+$ T cells	$[2e-1,\ 5e-1]$	Estimated
ω_h	Growth rate of $CD4^+$ T cells	$[8e-3,\ 3e-2]$	Estimated
ω_B	Growth rate of B cells	$[7.5e-2,\ 1.2e-1]$	Estimated
π_k	Carrying capacity of $CD8^+$ T cells	0.3	[21,39]
π_h	Carrying capacity of $CD4^+$ T cells	9	[21,39]
π_B	Carrying capacity of B cells	211	[28]
γ_k	Differentiation rate of memory $CD8^+$ T cells	/	/
γ_h	Differentiation rate of memory $CD4^+$ T cells	/	/
γ_B	Differentiation rate of memory B cells	/	/
η_k	Proliferation rate of memory $CD8^+$ T cells	/	/
η_h	Proliferation rate of memory $CD4^+$ T cells	/	/
η_B	Proliferation rate of memory B cells	/	/
δ_k	Apoptosis rate of memory $CD8^+$ T cells	/	/
δ_h	Apoptosis rate of memory $CD4^+$ T cells	/	/
δ_B	Apoptosis rate of memory B cells	/	/
μ_k	Ratio of effect of memory $CD8^+$ T cells	/	/
μ_h	Ratio of effect of memory $CD4^+$ T cells	/	/
μ_B	Ratio of effect of memory B cells	/	/

$$= \left(0, 0, 0, \pi_k, \pi_h, \pi_B, 0, \frac{\gamma_k \pi_k}{\delta_k}, \frac{\gamma_h \pi_h}{\delta_h}, \frac{\gamma_B \pi_B}{\delta_B}\right)^T,$$

$$\boldsymbol{E_2}(I_1, I_2, S, T_k, T_h, B, A, T_{km}, T_{hm}, B_m)$$

$$= \left(0, 0, 0, 0, \pi_h, \pi_B, 0, 0, \frac{\gamma_h \pi_h}{\delta_h}, \frac{\gamma_B \pi_B}{\delta_B}\right)^T,$$

$$\boldsymbol{E_3}(I_1, I_2, S, T_k, T_h, B, A, T_{km}, T_{hm}, B_m) = \left(0, 0, 0, \pi_k, 0, \pi_B, 0, \frac{\gamma_k \pi_k}{\delta_k}, 0, \frac{\gamma_B \pi_B}{\delta_B}\right)^T,$$

$$\boldsymbol{E_4}(I_1, I_2, S, T_k, T_h, B, A, T_{km}, T_{hm}, B_m) = \left(0, 0, 0, \pi_k, \pi_h, 0, 0, \frac{\gamma_k \pi_k}{\delta_k}, \frac{\gamma_h \pi_h}{\delta_h}, 0\right)^T,$$

$$\boldsymbol{E_5}(I_1, I_2, S, T_k, T_h, B, A, T_{km}, T_{hm}, B_m) = \left(0, 0, 0, \pi_k, 0, 0, 0, \frac{\gamma_k \pi_k}{\delta_k}, 0, 0\right)^T,$$

$$\boldsymbol{E_6}(I_1, I_2, S, T_k, T_h, B, A, T_{km}, T_{hm}, B_m) = \left(0, 0, 0, 0, \pi_h, 0, 0, 0, \frac{\gamma_h \pi_h}{\delta_h}, 0\right)^T,$$

$$\boldsymbol{E_7}(I_1, I_2, S, T_k, T_h, B, A, T_{km}, T_{hm}, B_m) = \left(0, 0, 0, 0, 0, \pi_B, 0, 0, 0, \frac{\gamma_B \pi_B}{\delta_B}\right)^T,$$

$$\boldsymbol{E_8}(I_1, I_2, S, T_k, T_h, B, A, T_{km}, T_{hm}, B_m) = (0, 0, 0, 0, 0, 0, 0, 0, 0, 0)^T.$$

We obtain the following conclusion about these equilibria.

Theorem 2.1. *In the case of a single vaccination, the disease-free equilibrium of four systems of vaccination* **Model 1-Model 4**

$$\begin{aligned}&\boldsymbol{E_1}(I_1, I_2, S, T_k, T_h, B, A, T_{km}, T_{hm}, B_m)\\ =&\left(0, 0, 0, \pi_k, \pi_h, \pi_B, 0, \frac{\gamma_k \pi_k}{\delta_k}, \frac{\gamma_h \pi_h}{\delta_h}, \frac{\gamma_B \pi_B}{\delta_B}\right)^T\end{aligned}$$

is unconditionally globally asymptotically stable, while the other equilibria $\boldsymbol{E_i}(i = 2, \ldots, 8)$ *are unstable.*

Proof. First, we prove it is locally asymptotically stable. For simplicity, denote

$$\boldsymbol{Z} = (I_1, I_2, S, T_k, T_h, B, A, T_{km}, T_{hm}, B_m)^T,$$

$$\boldsymbol{Y} = (I_1^*, I_2^*, S^*, T_k^*, T_h^*, B^*, A^*, T_{km}^*, T_{hm}^*, B_m^*)^T = \boldsymbol{Z} + \boldsymbol{E_1},$$

and we get a transformed model

$$\begin{cases}
\dfrac{dI_1^*}{dt} &= -\lambda\pi_k I_1^* - \dfrac{\lambda\mu_k\gamma_k\pi_k}{\delta_k} I_1^* - \delta_I I_1^* - \lambda\mu_k I_1^* T_{km}^* - \lambda I_1^* T_k^*,\\
\dfrac{dI_2^*}{dt} &= -\lambda\pi_k I_2^* - \dfrac{\lambda\mu_k\gamma_k\pi_k}{\delta_k} I_2^* - \delta_I I_2^* + \theta_1 S^* - \lambda\mu_k I_2^* T_{km}^* - \lambda I_2^* T_k^*,\\
\dfrac{dS^*}{dt} &= pI_1^* - \theta_1 S^* - \theta_2 S^* - \beta S^* A^*,\\
\dfrac{dT_k^*}{dt} &= \alpha_k I_1^* + \alpha_k I_2^* - \omega_k\pi_k T_k^* - \omega_k T_k^{*2},\\
\dfrac{dT_h^*}{dt} &= \alpha_h S^* - \omega_h\pi_h T_h^* - \omega_h T_h^{*2},\\
\dfrac{dB^*}{dt} &= \alpha_B\pi_h S^* + \dfrac{\alpha_B\mu_h\gamma_h\pi_h}{\delta_h} S^* - \omega_B\pi_B B^* - \omega_B B^{*2} + \alpha_B\mu_h S^* T_{hm}^*\\
&\quad + \alpha_B S^* T_h^*,\\
\dfrac{dA^*}{dt} &= \omega_A\pi_B S^* + \dfrac{\omega_A\mu_B\gamma_B\pi_B}{\delta_B} S^* - \delta_A A^* + \omega_A\mu_B S^* B_m^* + \omega_A S^* B^* - \beta S^* A^*,\\
\dfrac{dT_{km}^*}{dt} &= \dfrac{\eta_k\gamma_k\pi_k}{\delta_k} I_1^* + \dfrac{\eta_k\gamma_k\pi_k}{\delta_k} I_2^* + \gamma_k T_k^* - \delta_k T_{km}^* + \eta_k T_{km}^* I_1^* + \eta_k T_{km}^* I_2^*,\\
\dfrac{dT_{hm}^*}{dt} &= \dfrac{\eta_h\gamma_h\pi_h}{\delta_h} S^* + \gamma_h T_h^* - \delta_h T_{hm}^* + \eta_h T_{hm}^* S^*,\\
\dfrac{dB_m^*}{dt} &= \dfrac{\eta_B\gamma_B\pi_B}{\delta_B} S^* + \gamma_B B^* - \delta_B B_m^* + \eta_B B_m^* S^*.
\end{cases} \tag{8.1}$$

So the disease-free equilibrium $\boldsymbol{E_1}$ of the system (2.1) & (2.2) is equivalent to the equilibrium $\mathbf{0}$ of the system (8.1), and they have the same stability. It is easy to write the coefficient matrix of the linearized system of the system (8.1) at $\mathbf{0}$ as follows:

$$\begin{pmatrix}
-a_1 & 0 & 0 & 0 & 0 & 0 & 0 & 0 & 0 & 0 \\
0 & -a_1 & \theta_1 & 0 & 0 & 0 & 0 & 0 & 0 & 0 \\
p & 0 & -(\theta_1+\theta_2) & 0 & 0 & 0 & 0 & 0 & 0 & 0 \\
\alpha_k & \alpha_k & 0 & -\omega_k\pi_k & 0 & 0 & 0 & 0 & 0 & 0 \\
0 & 0 & \alpha_h & 0 & -\omega_h\pi_h & 0 & 0 & 0 & 0 & 0 \\
0 & 0 & a_2 & 0 & 0 & -\omega_B\pi_B & 0 & 0 & 0 & 0 \\
0 & 0 & a_3 & 0 & 0 & 0 & -\delta_A & 0 & 0 & 0 \\
\dfrac{\eta_k\gamma_k\pi_k}{\delta_k} & \dfrac{\eta_k\gamma_k\pi_k}{\delta_k} & 0 & \gamma_k & 0 & 0 & 0 & -\delta_k & 0 & 0 \\
0 & 0 & \dfrac{\eta_h\gamma_h\pi_h}{\delta_h} & 0 & \gamma_h & 0 & 0 & 0 & -\delta_h & 0 \\
0 & 0 & \dfrac{\eta_B\gamma_B\pi_B}{\delta_B} & 0 & 0 & \gamma_B & 0 & 0 & 0 & -\delta_B
\end{pmatrix}$$

where, $a_1 = \lambda\pi_k + \frac{\lambda\mu_k\gamma_k\pi_k}{\delta_k} + \delta_I, a_2 = \alpha_B\pi_h + \frac{\alpha_B\mu_h\gamma_h\pi_h}{\delta_h}, a_3 = \omega_A\pi_B + \frac{\omega_A\mu_B\gamma_B\pi_B}{\delta_B}$.

We can get its characteristic equation

$$(\lambda^*+a_1)^2(\lambda^*+\theta_1+\theta_2)(\lambda^*+\omega_k\pi_k)(\lambda^*+\omega_h\pi_h)(\lambda^*+\omega_B\pi_B)(\lambda^*+\delta_A) \times(\lambda^*+\delta_k)(\lambda^*+\delta_h)(\lambda^*+\delta_B)=0.$$

Since the parameters are all positive real numbers, the eigenvalues are all negative real numbers, so it can be known that the zero solution of (8.1) is locally asymptotically stable, i.e., the disease-free equilibrium $\boldsymbol{E_1}$ of (2.1) & (2.2) is locally asymptotically stable.

Then we prove that $\boldsymbol{E_1}$ is globally attractive. Denote the space

$$\mathbf{U} = R^* \times R^* \times R^* \times R^+ \times R^+ \times R^+ \times R^* \times R^* \times R^* \times R^*,$$

where, R^+ denotes all positive real numbers, and $R^* = R^+ \cup \{0\}$. The following shows that the domain of attraction of $\boldsymbol{E_1}$ is $\mathbf{U}$ by analyzing the equations one by one of the original system (2.1) & (2.2).

First, we take arbitrary $\boldsymbol{x}(t_0) \in \mathbf{U}$, and denote $\boldsymbol{x}(t_i) = (I_1^{(i)}, I_2^{(i)}, S^{(i)}, T_k^{(i)}, T_h^{(i)}, B^{(i)}, A^{(i)}, T_{km}^{(i)}, T_{hm}^{(i)}, B_m^{(i)})^T$ the point when $t = t_i$ when the system started from $\boldsymbol{x}(t_0)$.

I Considering

$$\frac{dI_1}{dt} = -\delta_I I_1 - \lambda I_1(T_k + \mu_k T_{km}) \le -\delta_I I_1.$$

Then,

$$I_1 \le I_1^{(0)} e^{-\delta_I(t-t_0)} \triangleq x_1(t).$$

So, for x_1, for $\forall\epsilon_1 \in (0, I_1^{(0)}], \exists t_1 = t_0 - \frac{1}{\delta_I}\ln\frac{\epsilon_1}{I_1^{(0)}} \ge t_0, s.t. \forall t > t_1, ||x_1(t)|| < \epsilon_1$.

Also, because $\frac{dI_1}{dt}|_{I_1=0} = 0$, we can know $I_1 \ge 0$, so, $||I_1(t)|| < \epsilon_1$ when $t > t_1$.

II When $t \geq t_1$, considering

$$\frac{dS}{dt} = pI_1 - (\theta_1 + \theta_2)S - \beta SA \leq p\epsilon_1 - (\theta_1 + \theta_2)S.$$

Then,

$$\begin{aligned} S &\leq \frac{p\epsilon_1}{\theta_1 + \theta_2} + (S^{(1)} - \frac{p\epsilon_1}{\theta_1 + \theta_2})e^{-(\theta_1+\theta_2)(t-t_1)} \\ &\leq \frac{p\epsilon_1}{\theta_1 + \theta_2} + S^{(1)}e^{-(\theta_1+\theta_2)(t-t_1)} \triangleq x_2(t). \end{aligned}$$

So, for x_2, for $\forall \epsilon_2 > 0$, we define arbitrary small positive numbers $\epsilon_1 < \min\{\frac{(\theta_1+\theta_2)\epsilon_2}{p}, I_1^{(0)}\}$, and we get $\exists t_2 = t_1 - \frac{1}{\theta_1+\theta_2}\ln(\frac{\epsilon_2}{S^{(1)}} - \frac{p\epsilon_1}{S^{(1)}(\theta_1+\theta_2)}) > t_1, s.t. \forall t > t_2, ||x_2(t)|| < \epsilon_2$. Obviously, $S \geq 0$, so $||S(t)|| < \epsilon_2$ when $t > t_2$.

III When $t \geq t_2$, considering

$$\frac{dI_2}{dt} = \theta_1 S - \delta_I I_2 - \lambda I_2(T_k + \mu_k T_{km}) \leq \theta_1\epsilon_2 - \delta_I I_2.$$

Then,

$$I_2 \leq \frac{\theta_1\epsilon_2}{\delta_I} + (I_2^{(2)} - \frac{\theta_1\epsilon_2}{\delta_I})e^{-\delta_I(t-t_2)} \leq \frac{\theta_1\epsilon_2}{\delta_I} + I_2^{(2)}e^{-\delta_I(t-t_2)} \triangleq x_3(t).$$

So, for x_3, for $\forall \epsilon_3 > 0$, we define arbitrary small positive numbers $\epsilon_2 < \frac{\delta_I\epsilon_3}{\theta_1}, \epsilon_1 < \min\{\frac{(\theta_1+\theta_2)\epsilon_2}{p}, I_1^{(0)}\}$, and we get $\exists t_3 = t_2 - \frac{1}{\delta_I}\ln(\frac{\epsilon_3}{I_2^{(2)}} - \frac{\theta_1\epsilon_2}{I_2^{(2)}\delta_I}) > t_2, s.t. \forall t > t_3, ||x_3(t)|| < \epsilon_3$. Obviously, $I_2 \geq 0$, so $||I_2(t)|| < \epsilon_3$ when $t > t_3$.

IV When $t \geq t_3$, considering

$$\frac{dT_k}{dt} = \alpha_k(I_1 + I_2) + \omega_k\pi_k T_k - \omega_k T_k^2 \leq \alpha_k(\epsilon_1 + \epsilon_3) + \omega_k\pi_k T_k - \omega_k T_k^2.$$

Then,

$$T_k \leq \frac{\tanh\left[\frac{(t-t_3)G_1}{2} + \operatorname{arctanh}\left(\frac{\omega_k(2T_k^{(3)} - \pi_k)}{G_1}\right)\right]G_1 + \omega_k\pi_k}{2\omega_k} \triangleq x_4^{(u)}(t),$$

where, $G_1 = \sqrt{\omega_k(\omega_k\pi_k^2 + 4\alpha_k(\epsilon_1 + \epsilon_3))}$.
It is easy to know $x_4^{(u)}(t) - \pi_k \leq \frac{G_1 + \omega_k\pi_k}{2\omega_k} - \pi_k$.
On the other hand, considering

$$\frac{dT_k}{dt} \geq \omega_k\pi_k T_k - \omega_k T_k^2.$$

Then,

$$T_k \geq \frac{T_k^{(3)}\pi_k e^{\omega_k\pi_k(t-t_3)}}{T_k^{(3)}e^{\omega_k\pi_k(t-t_3)} + \pi_k - T_k^{(3)}} \triangleq x_4^{(l)}(t).$$

Obviously, $\forall \epsilon_4^* > 0, \exists T_4 > t_3, s.t. \forall t > T_4, |e^{\omega_k\pi_k(t-t_3)}| > \frac{1}{\epsilon_4^*}$ and
$|\tanh\left[\frac{(t-t_3)G_1}{2} + \operatorname{arctanh}\left(\frac{\omega_k(2T_k^{(3)} - \pi_k)}{G_1}\right)\right] - 1| < \epsilon_4^*$.

So, for $x_4^{(u)}$ and $x_4^{(l)}$, for $\forall \epsilon_4 > 0$, we define arbitrary small positive numbers $\epsilon_1 + \epsilon_3 < \frac{\omega_k \epsilon_4}{\alpha_k}(\pi_k + \epsilon_4), \epsilon_2 < \frac{\delta_I \epsilon_3}{\theta_1}, \epsilon_1 < \min\{\frac{(\theta_1+\theta_2)\epsilon_2}{p}, I_1^{(0)}\}$, and we get $\exists t_4 > T_4, s.t. \forall t > t_4, ||x_4^{(u)}(t) - \pi_k|| < \epsilon_4, ||x_4^{(l)}(t) - \pi_k|| < \epsilon_4$. so $||T_k(t) - \pi_k|| < \epsilon_4$ when $t > t_4$.

V When $t \geq t_4$, considering

$$\frac{dT_h}{dt} = \alpha_h S + \omega_h \pi_h T_h - \omega_h T_h^2 \leq \alpha_h \epsilon_2 + \omega_h \pi_h T_h - \omega_h T_h^2.$$

Then,

$$T_h \leq \frac{\tanh\left[\frac{(t-t_4)G_2}{2} + \operatorname{arctanh}\left(\frac{\omega_h(2T_h^{(4)} - \pi_h)}{G_2}\right)\right] G_2 + \omega_h \pi_h}{2\omega_h} \triangleq x_5^{(u)}(t),$$

where, $G_2 = \sqrt{\omega_h(\omega_h \pi_h^2 + 4\alpha_h \epsilon_2)}$.
It is easy to know $x_5^{(u)}(t) - \pi_h \leq \frac{G_2 + \omega_h \pi_h}{2\omega_h} - \pi_h$.
On the other hand, considering

$$\frac{dT_h}{dt} \geq \omega_h \pi_h T_h - \omega_h T_h^2.$$

Then,

$$T_h \geq \frac{T_h^{(4)} \pi_h e^{\omega_h \pi_h (t-t_4)}}{T_h^{(4)} e^{\omega_h \pi_h (t-t_4)} + \pi_h - T_h^{(4)}} \triangleq x_5^{(l)}(t).$$

Similar to IV, for $x_5^{(u)}$ and $x_5^{(l)}$, for $\forall \epsilon_5 > 0$, we define arbitrary small positive numbers $\epsilon_4 > 0, \epsilon_1 + \epsilon_3 < \frac{\omega_k \epsilon_4}{\alpha_k}(\pi_k + \epsilon_4), \epsilon_2 < \min\{\frac{\omega_h \epsilon_5}{\alpha_h}(\pi_h + \epsilon_5), \frac{\delta_I \epsilon_3}{\theta_1}\}, \epsilon_1 < \min\{\frac{(\theta_1+\theta_2)\epsilon_2}{p}, I_1^{(0)}\}$, and we get $\exists t_5 > t_4, s.t. \forall t > t_5, ||x_5^{(u)}(t) - \pi_h|| < \epsilon_5$, $||x_5^{(l)}(t) - \pi_h|| < \epsilon_5$. So $||T_h(t) - \pi_h|| < \epsilon_5$ when $t > t_5$.

VI When $t \geq t_5$, considering

$$\frac{dT_{km}}{dt} = \gamma_k T_k - \delta_k T_{km} + \eta_k T_{km}(I_1 + I_2) \leq \gamma_k(\pi_k + \epsilon_4) - (\delta_k - \eta_k(\epsilon_1 + \epsilon_3))T_{km}.$$

Then,

$$\begin{aligned} T_{km} &\leq \frac{\gamma_k(\pi_k + \epsilon_4)}{\delta_k - \eta_k(\epsilon_1 + \epsilon_3)} + (T_{km}^{(5)} - \frac{\gamma_k(\pi_k + \epsilon_4)}{\delta_k - \eta_k(\epsilon_1 + \epsilon_3)}) e^{-(\delta_k - \eta_k(\epsilon_1+\epsilon_3))(t-t_5)} \\ &\triangleq x_6^{(u)}(t). \end{aligned}$$

On the other hand, considering

$$\frac{dT_{km}}{dt} \geq \gamma_k(\pi_k - \epsilon_4) - \delta_k T_{km}.$$

Then,

$$T_{km} \geq \frac{\gamma_k(\pi_k - \epsilon_4)}{\delta_k} + (T_{km}^{(5)} - \frac{\gamma_k(\pi_k - \epsilon_4)}{\delta_k}) e^{-\delta_k(t-t_5)} \triangleq x_6^{(l)}(t).$$

So, for $x_6^{(u)}$ and $x_6^{(l)}$, for $\forall\epsilon_6 > 0$, we define arbitrary small positive numbers $\epsilon_5 > 0$, $\frac{\gamma_k[\delta_k\epsilon_4+\pi_k\eta_k(\epsilon_1+\epsilon_3)]}{\delta_k[\delta_k-\eta_k(\epsilon_1+\epsilon_3)]} < \epsilon_6, \epsilon_4 < \frac{\delta_k\epsilon_6}{\gamma_k}, \epsilon_1+\epsilon_3 < \min\{\frac{\delta_k}{\eta_k}, \frac{\omega_k\epsilon_4}{\alpha_k}(\pi_k+\epsilon_4)\}, \epsilon_2 < \min\{\frac{\omega_h\epsilon_5}{\alpha_h}(\pi_h+\epsilon_5), \frac{\delta_I\epsilon_3}{\theta_1}\}$, $\epsilon_1 < \min\{\frac{(\theta_1+\theta_2)\epsilon_2}{p}, I_1^{(0)}\}$, and we get $\exists t_6 > t_5$, $s.t.\forall t > t_6, ||x_6^{(u)}(t) - \frac{\gamma_k\pi_k}{\delta_k}|| < \epsilon_6, ||x_6^{(l)}(t) - \frac{\gamma_k\pi_k}{\delta_k}|| < \epsilon_6$. So $||T_{km}(t) - \frac{\gamma_k\pi_k}{\delta_k}|| < \epsilon_6$ when $t > t_6$.

VII When $t \geq t_6$, considering

$$\frac{dT_{hm}}{dt} = \gamma_h T_h - \delta_h T_{hm} + \eta_h T_{hm} S \leq \gamma_h(\pi_h+\epsilon_5) - (\delta_h - \eta_h\epsilon_2)T_{hm}.$$

Then,

$$T_{hm} \leq \frac{\gamma_h(\pi_h+\epsilon_5)}{\delta_h-\eta_h\epsilon_2} + (T_{hm}^{(6)} - \frac{\gamma_h(\pi_h+\epsilon_5)}{\delta_h-\eta_h\epsilon_2})e^{-(\delta_h-\eta_h\epsilon_2)(t-t_6)} \triangleq x_7^{(u)}(t).$$

On the other hand, considering

$$\frac{dT_{hm}}{dt} \geq \gamma_h(\pi_h-\epsilon_5) - \delta_h T_{hm}.$$

Then,

$$T_{hm} \geq \frac{\gamma_h(\pi_h-\epsilon_5)}{\delta_h} + (T_{hm}^{(6)} - \frac{\gamma_h(\pi_h-\epsilon_5)}{\delta_h})e^{-\delta_h(t-t_6)} \triangleq x_7^{(l)}(t).$$

So, for $x_7^{(u)}$ and $x_7^{(l)}$, for $\forall\epsilon_7 > 0$, we define arbitrary small positive numbers $\frac{\gamma_h[\delta_h\epsilon_5+\pi_h\eta_h\epsilon_2]}{\delta_h(\delta_h-\eta_h\epsilon_2)} < \epsilon_7, \epsilon_5 < \frac{\delta_h\epsilon_7}{\gamma_h}, \frac{\gamma_k[\delta_k\epsilon_4+\pi_k\eta_k(\epsilon_1+\epsilon_3)]}{\delta_k[\delta_k-\eta_k(\epsilon_1+\epsilon_3)]} < \epsilon_6, \epsilon_4 < \frac{\delta_k\epsilon_6}{\gamma_k}, \epsilon_1+\epsilon_3 < \min\{\frac{\delta_k}{\eta_k}, \frac{\omega_k\epsilon_4}{\alpha_k}(\pi_k+\epsilon_4)\}, \epsilon_2 < \min\{\frac{\delta_h}{\eta_h}, \frac{\omega_h\epsilon_5}{\alpha_h}(\pi_h+\epsilon_5), \frac{\delta_I\epsilon_3}{\theta_1}\}, \epsilon_1 < \min\{\frac{(\theta_1+\theta_2)\epsilon_2}{p}, I_1^{(0)}\}$, and we get $\exists t_7 > t_6, s.t.\forall t > t_7, ||x_7^{(u)}(t) - \frac{\gamma_h\pi_h}{\delta_h}|| < \epsilon_7, ||x_7^{(l)}(t) - \frac{\gamma_h\pi_h}{\delta_h}|| < \epsilon_7$. So $||T_{hm}(t) - \frac{\gamma_h\pi_h}{\delta_h}|| < \epsilon_7$ when $t > t_7$.

VIII When $t \geq t_7$, considering

$$\begin{aligned}\frac{dB}{dt} &= \alpha_B S(T_h + \mu_h T_{hm}) + \omega_B\pi_B B - \omega_B B^2 \\ &\leq \alpha_B\epsilon_2(\pi_h+\epsilon_5+\mu_h(\frac{\gamma_h\pi_h}{\delta_h}+\epsilon_7)) + \omega_B\pi_B B - \omega_B B^2.\end{aligned}$$

Then,

$$\begin{aligned}B &\leq \frac{\pi_B}{2} + \frac{1}{2\omega_B\delta_h}\tanh\left[\frac{(t-t_7)G_3}{2\delta_h} + \operatorname{arctanh}\left(\frac{\delta_h\omega_B(2B^{(7)}-\pi_B)}{G_3}\right)\right]G_3 \\ &\triangleq x_8^{(u)}(t),\end{aligned}$$

where, $G_3 = \sqrt{\omega_B\delta_h(4\alpha_B\epsilon_2(\delta_h(\mu_h\epsilon_7+\pi_h+\epsilon_5)+\mu_h\pi_h\gamma_h)+\omega_B\pi_B^2\delta_h)}$.
On the other hand, considering

$$\frac{dB}{dt} \geq \omega_B\pi_B B - \omega_B B^2.$$

Then,

$$B \geq \frac{B^{(7)}\pi_B e^{\omega_B\pi_B(t-t_7)}}{B^{(7)}e^{\omega_B\pi_B(t-t_7)} + \pi_B - B^{(7)}} \triangleq x_8^{(l)}(t).$$

So, for $x_8^{(u)}$ and $x_8^{(l)}$, for $\forall\epsilon_8 > 0$, we define arbitrary small positive numbers $\frac{\alpha_B\epsilon_2}{\omega_B\delta_h}[\delta_h(\mu_h\epsilon_7+\pi_h+\epsilon_5)+\mu_h\pi_h\gamma_h] < \epsilon_8(\pi_B+\epsilon_8)$, $\frac{\gamma_h[\delta_h\epsilon_5+\pi_h\eta_h\epsilon_2]}{\delta_h(\delta_h-\eta_h\epsilon_2)} < \epsilon_7, \epsilon_5 < \frac{\delta_h\epsilon_7}{\gamma_h}$, $\frac{\gamma_k[\delta_k\epsilon_4+\pi_k\eta_k(\epsilon_1+\epsilon_3)]}{\delta_k[\delta_k-\eta_k(\epsilon_1+\epsilon_3)]} < \epsilon_6, \epsilon_4 < \frac{\delta_k\epsilon_6}{\gamma_k}, \epsilon_1+\epsilon_3 < \min\{\frac{\delta_k}{\eta_k}, \frac{\omega_k\epsilon_4}{\alpha_k}(\pi_k+\epsilon_4)\}, \epsilon_2 < \min\{\frac{\delta_h}{\eta_h}, \frac{\omega_h\epsilon_5}{\alpha_h}(\pi_h+\epsilon_5), \frac{\delta_I\epsilon_3}{\theta_1}\}, \epsilon_1 < \min\{\frac{(\theta_1+\theta_2)\epsilon_2}{p}, I_1^{(0)}\}$, and we get $\exists t_8 > t_7, s.t. \forall t > t_8, ||x_8^{(u)}(t)-\pi_B|| < \epsilon_8, ||x_8^{(l)}(t)-\pi_B|| < \epsilon_8$. So $||B(t)-\pi_B|| < \epsilon_8$ when $t > t_8$.

IX When $t \geq t_8$, considering

$$\frac{dB_m}{dt} = \gamma_B B - \delta_B B_m + \eta_B B_m S \leq \gamma_B(\pi_B+\epsilon_8) - (\delta_B - \eta_B\epsilon_2)B_m.$$

Then,

$$B_m \leq \frac{\gamma_B(\pi_B+\epsilon_8)}{\delta_B-\eta_B\epsilon_2} + (B_m^{(8)} - \frac{\gamma_B(\pi_B+\epsilon_8)}{\delta_B-\eta_B\epsilon_2})e^{-(\delta_B-\eta_B\epsilon_2)(t-t_8)} \triangleq x_9^{(u)}(t).$$

On the other hand, considering

$$\frac{dB_m}{dt} \geq \gamma_B(\pi_B-\epsilon_8) - \delta_B B_m.$$

Then,

$$B_m \geq \frac{\gamma_B(\pi_B-\epsilon_8)}{\delta_B} + (B_m^{(8)} - \frac{\gamma_B(\pi_B-\epsilon_8)}{\delta_B})e^{-\delta_B(t-t_8)} \triangleq x_9^{(l)}(t).$$

So, for $x_9^{(u)}$ and $x_9^{(l)}$, for $\forall\epsilon_9 > 0$, we define arbitrary small positive numbers $\frac{\gamma_B[\delta_B\epsilon_8+\pi_B\eta_B\epsilon_2]}{\delta_B(\delta_B-\eta_B\epsilon_2)} < \epsilon_9, \epsilon_8 < \frac{\delta_B\epsilon_9}{\gamma_B}$, $\frac{\alpha_B\epsilon_2[\delta_h(\mu_h\epsilon_7+\pi_h+\epsilon_5)+\mu_h\pi_h\gamma_h]}{\omega_B\delta_h} < \epsilon_8(\pi_B+\epsilon_8)$, $\frac{\gamma_h[\delta_h\epsilon_5+\pi_h\eta_h\epsilon_2]}{\delta_h(\delta_h-\eta_h\epsilon_2)} < \epsilon_7, \epsilon_5 < \frac{\delta_h\epsilon_7}{\gamma_h}$, $\frac{\gamma_k[\delta_k\epsilon_4+\pi_k\eta_k(\epsilon_1+\epsilon_3)]}{\delta_k[\delta_k-\eta_k(\epsilon_1+\epsilon_3)]} < \epsilon_6, \epsilon_4 < \frac{\delta_k\epsilon_6}{\gamma_k}, \epsilon_1+\epsilon_3 < \min\{\frac{\delta_k}{\eta_k}, \frac{\omega_k\epsilon_4}{\alpha_k}(\pi_k+\epsilon_4)\}, \epsilon_2 < \min\{\frac{\delta_B}{\eta_B}, \frac{\delta_h}{\eta_h}, \frac{\omega_h\epsilon_5}{\alpha_h}(\pi_h+\epsilon_5), \frac{\delta_I\epsilon_3}{\theta_1}\}, \epsilon_1 < \min\{\frac{(\theta_1+\theta_2)\epsilon_2}{p}, I_1^{(0)}\}$, and we get $\exists t_9 > t_8, s.t. \forall t > t_9, ||x_9^{(u)}(t) - \frac{\gamma_B\pi_B}{\delta_B}|| < \epsilon_9, ||x_9^{(l)}(t) - \frac{\gamma_B\pi_B}{\delta_B}|| < \epsilon_9$. So $||B_m(t) - \frac{\gamma_B\pi_B}{\delta_B}|| < \epsilon_9$ when $t > t_9$.

X When $t \geq t_9$, considering

$$\frac{dA}{dt} = -\delta_A A - \beta SA + \omega_A S(B+\mu_B B_m) \leq \omega_A\epsilon_2(\pi_B+\epsilon_8+\mu_B(\frac{\gamma_B\pi_B}{\delta_B}+\epsilon_9)) - \delta_A A.$$

Then,

$$A \leq \frac{G_4}{\delta_A} + (A^{(9)} - \frac{G_4}{\delta_A})e^{-\delta_A(t-t_9)} \triangleq x_{10}(t).$$

where, $G_4 = \omega_A\epsilon_2(\pi_B+\epsilon_8+\mu_B(\frac{\gamma_B\pi_B}{\delta_B}+\epsilon_9))$.
So, for x_{10}, for $\forall\epsilon_{10} > 0$, we define arbitrary small positive numbers $\frac{\omega_A\epsilon_2(\pi_B+\epsilon_8+\mu_B(\frac{\gamma_B\pi_B}{\delta_B}+\epsilon_9))}{\delta_A} < \epsilon_{10}$, $\frac{\gamma_B[\delta_B\epsilon_8+\pi_B\eta_B\epsilon_2]}{\delta_B(\delta_B-\eta_B\epsilon_2)} < \epsilon_9, \epsilon_8 < \frac{\delta_B\epsilon_9}{\gamma_B}$, $\frac{\alpha_B\epsilon_2[\delta_h(\mu_h\epsilon_7+\pi_h+\epsilon_5)+\mu_h\pi_h\gamma_h]}{\omega_B\delta_h} < \epsilon_8(\pi_B+\epsilon_8)$, $\frac{\gamma_h[\delta_h\epsilon_5+\pi_h\eta_h\epsilon_2]}{\delta_h(\delta_h-\eta_h\epsilon_2)} < \epsilon_7, \epsilon_5 < \frac{\delta_h\epsilon_7}{\gamma_h}$, $\frac{\gamma_k[\delta_k\epsilon_4+\pi_k\eta_k(\epsilon_1+\epsilon_3)]}{\delta_k[\delta_k-\eta_k(\epsilon_1+\epsilon_3)]} < \epsilon_6, \epsilon_4 < \frac{\delta_k\epsilon_6}{\gamma_k}, \epsilon_1+\epsilon_3 < \min\{\frac{\delta_k}{\eta_k}, \frac{\omega_k\epsilon_4}{\alpha_k}(\pi_k+\epsilon_4)\}, \epsilon_2 < \min\{\frac{\delta_B}{\eta_B}, \frac{\delta_h}{\eta_h}, \frac{\omega_h\epsilon_5}{\alpha_h}(\pi_h+\epsilon_5), \frac{\delta_I\epsilon_3}{\theta_1}\}, \epsilon_1 < \min\{\frac{(\theta_1+\theta_2)\epsilon_2}{p}, I_1^{(0)}\}$, and we get $\exists t_{10} > t_9, s.t. \forall t > t_{10}, ||x_{10}(t)|| < \epsilon_{10}$. Obviously, $A \geq 0$, so $||A(t)|| < \epsilon_{10}$ when $t > t_{10}$.

Finally, it can be shown that the domain of attraction of $\boldsymbol{E_1}$ is $\mathbf{U}$. So, $\boldsymbol{E_1}$ is unconditionally globally asymptotically stable.

For equilibria $\boldsymbol{E_i}(i = 2, \ldots, 8)$, we also perform the corresponding translational transformations of the original system, making the equilibria be $\mathbf{0}$ after transformations. Now we can calculate the characteristics equations of the coefficient matrices of the linearized systems of the transformed systems at $\mathbf{0}$, and they are displayed sequentially as follows:

$$
\begin{aligned}
&(\lambda^* + \delta_I)^2(\lambda^* + \theta_1 + \theta_2)(\lambda^* - \omega_k\pi_k)(\lambda^* + \omega_h\pi_h)(\lambda^* + \omega_B\pi_B)(\lambda^* + \delta_A)\\
&\times(\lambda^* + \delta_k)(\lambda^* + \delta_h)(\lambda^* + \delta_B) = 0,\\
&(\lambda^* + a_1)^2(\lambda^* + \theta_1 + \theta_2)(\lambda^* + \omega_k\pi_k)(\lambda^* - \omega_h\pi_h)(\lambda^* + \omega_B\pi_B)(\lambda^* + \delta_A)\\
&\times(\lambda^* + \delta_k)(\lambda^* + \delta_h)(\lambda^* + \delta_B) = 0,\\
&(\lambda^* + a_1)^2(\lambda^* + \theta_1 + \theta_2)(\lambda^* + \omega_k\pi_k)(\lambda^* + \omega_h\pi_h)(\lambda^* - \omega_B\pi_B)(\lambda^* + \delta_A)\\
&\times(\lambda^* + \delta_k)(\lambda^* + \delta_h)(\lambda^* + \delta_B) = 0,\\
&(\lambda^* + a_1)^2(\lambda^* + \theta_1 + \theta_2)(\lambda^* + \omega_k\pi_k)(\lambda^* - \omega_h\pi_h)(\lambda^* - \omega_B\pi_B)(\lambda^* + \delta_A)\\
&\times(\lambda^* + \delta_k)(\lambda^* + \delta_h)(\lambda^* + \delta_B) = 0,\\
&(\lambda^* + \delta_I)^2(\lambda^* + \theta_1 + \theta_2)(\lambda^* - \omega_k\pi_k)(\lambda^* + \omega_h\pi_h)(\lambda^* - \omega_B\pi_B)(\lambda^* + \delta_A)\\
&\times(\lambda^* + \delta_k)(\lambda^* + \delta_h)(\lambda^* + \delta_B) = 0,\\
&(\lambda^* + \delta_I)^2(\lambda^* + \theta_1 + \theta_2)(\lambda^* - \omega_k\pi_k)(\lambda^* - \omega_h\pi_h)(\lambda^* + \omega_B\pi_B)(\lambda^* + \delta_A)\\
&\times(\lambda^* + \delta_k)(\lambda^* + \delta_h)(\lambda^* + \delta_B) = 0,\\
&(\lambda^* + \delta_I)^2(\lambda^* + \theta_1 + \theta_2)(\lambda^* - \omega_k\pi_k)(\lambda^* - \omega_h\pi_h)(\lambda^* - \omega_B\pi_B)(\lambda^* + \delta_A)\\
&\times(\lambda^* + \delta_k)(\lambda^* + \delta_h)(\lambda^* + \delta_B) = 0,
\end{aligned}
$$

where, $a_1 = \lambda\pi_k + \frac{\lambda\mu_k\gamma_k\pi_k}{\delta_k} + \delta_I$. Obviously, they all have at least one positive characteristic root, so these equilibria are unstable. □

Appendix B. Data

Z. Zhang's team from the La Jolla Institute for Immunology (USA) injected two groups of 30 adults primarily composed of white individuals with mRNA-1273 at a dose of $100\mu g$ and BNT162b2 at a dose of $30\mu g$, with the subjects receiving two doses of the vaccine at about 4 weeks intervals [39]. The immune cells were measured before the first vaccination, 2 weeks, 1 month, 3.5 months, and 6 months after the first vaccination. The geometric mean of the number of subsets of immune cells of interest was obtained. These numbers of subsets of the $CD8^+$ T cells and the $CD4^+$ T cells are used in our fitting, and the results of the fitting are then used to evaluate the different models to determine which one is more appropriate for this clinical dataset.

R. R. Goel's team from the University of Pennsylvania vaccinated 3 adult subjects with mRNA-1273 and 42 adult subjects with BNT162b2. The interval between the two vaccinations was 4 weeks. Clinical data were collected before the first dose, 2 weeks, 4 weeks, 5 weeks, 3 months, and 6 months after the first dose, and a time series of the numbers of specific subsets of memory cells was given for each subject. The team found that the mRNA vaccine induced durable immune memory. The data of the memory $CD8^+$ T cells, the memory $CD4^+$ T cells, and the memory B cells in our model were taken from the literature [13].

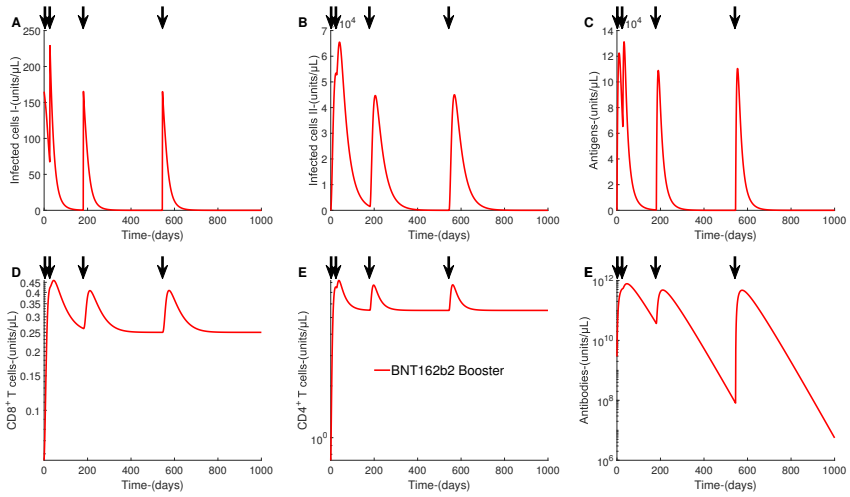

Figure 7. Injection of BNT162b2 booster. The red lines show the dynamics after the boosters of BNT162b2. The arrows mark the time points one is injected.

C. Lucas's team from Yale University compared the impact of different variants of the viruses on the immunity induced by the mRNA vaccine by vaccinating 18 test subjects between November 2020 and January 2021. 11 adult subjects were vaccinated with mRNA-1273, and 7 adult subjects were vaccinated with BNT162b2. Vaccination intervals were again 4 weeks. The team measured the IgG neutralizing antibodies against S, S1, and RBD receptors before the first injection, and at 1, 4, 5, 8, and 70 days after the first injection. These antibodies are related to the antigens in our model. Data on neutralizing antibodies involved in the four models are taken from the literature [22].

Also, to make the results of the study more credible, we only chose the data from subjects who had not been infected with SARS-CoV-2 in the literature, to ensure that the data come from as similar a population as possible and that the doses of the same vaccine are the same. Finally, we extracted the data and further processes them so that they have the same units and scale.

Appendix C. Simulation of BNT162b2 booster

The simulation of BNT162b2 booster is shown in Figure 7.

References

[1] H. Akaike, *Statistical predictor identification*, Annals of the Institute of Statistical Mathematics, 1970, 22(1), 203–217.

[2] H. Akaike, *Information theory and an extension of the maximum likelihood principle*, Proceedings of the Second International Symposium on Information Theory, 1973, 267–281.

[3] H. Akaike, *A new look at the statistical model identification*, Automatic Control IEEE Transactions on Automatic Control, 1974, 19(6), 716–723.

[4] L. R. Baden, H. M. El Sahly, B. Essink, K. Kotloff, S. Frey, R. Novak, D. Diemert, S. A. Spector, N. Rouphael and C. B. Creech, *Efficacy and safety of the mRNA-1273 SARS-CoV-2 vaccine*, New England Journal of Medicine, 2021, 384(5), 403–416.

[5] G. Bellu, M. P. Saccomani, S. Audoly and L. D'Angiò, *Daisy: A new software tool to test global identifiability of biological and physiological systems*, Computer Methods and Programs in Biomedicine, 2007, 88(1), 52–61.

[6] S. P. Brooks and A. Gelman, *General methods for monitoring convergence of iterative simulations*, Journal of Computational and Graphical Statistics, 1998, 7(4), 434–455.

[7] M. Chen, Q. Shao and J. G. Ibrahim, *Monte Carlo Methods in Bayesian Computation*, Springer, 2000. DOI: 10.1007/978-1-4612-1276-8.

[8] M. S. Diamond and T. D. Kanneganti, *Innate immunity: The first line of defense against SARS-CoV-2*, Nature Immunology, 2022, 23(2), 165–176.

[9] N. D. Evans, L. J. White and M. J. Chapman, *The structural identifiability of the susceptible infected recovered model with seasonal forcing*, Mathematical Biosciences, 2005, 194(2), 175–197.

[10] A. Gelman and D. B. Rubin, *Inference from iterative simulation using multiple sequences*, Statistical Science, 1992, 7(4), 457–472.

[11] M. Gheblawi, K. Wang, A. Viveiros, Q. Nguyen, J. C. Zhong, A. J. Turner, M. K. Raizada, M. B. Grant and G. Y. Oudit, *Angiotensin-converting enzyme 2: SARS-CoV-2 receptor and regulator of the renin-angiotensin system: Celebrating the 20th anniversary of the discovery of ACE2*, Circulation Research, 2020, 126(10), 1456–1474.

[12] Ghosh, *Introduction to applied Bayesian statistics and estimation for social scientists by Scott M. Lynch*, International Statal Review, 2010, 76(2), 311–312.

[13] R. R. Goel, M. M. Painter, S. A. Apostolidis, D. Mathew, W. Meng, A. M. Rosenfeld, K. A. Lundgreen, A. Reynaldi, D. S. Khoury and A. Pattekar, *mRNA vaccines induce durable immune memory to SARS-CoV-2 and variants of concern*, Science, 2021. DOI: 10.1126/science.abm0829.

[14] J. Goodman and J. Weare, *Ensemble samplers with affine invariance*, Communications in Applied Mathematics and Computational Science, 2010, 5(1), 65–80.

[15] K. Hattaf and N. Yousfi, *Dynamics of SARS-CoV-2 infection model with two modes of transmission and immune response*, Mathematical Biosciences and Engineering, 2020, 17(5), 5326–5340.

[16] G. He and J. Wang, *Threshold dynamics of an epidemic model with latency and vaccination in a heterogeneous habitat*, Journal of Nonlinear Modeling and Analysis, 2020, 2(3), 393–410.

[17] D. M. Hinke, T. K. Andersen, R. P. Gopalakrishnan, L. M. Skullerud, I. C. Werninghaus, G. Grodeland, E. Fossum, R. Braathen and B. Bogen, *Antigen bivalency of antigen-presenting cell-targeted vaccines increases B cell responses*, Cell Reports, 2022, 39(9), 110901.

[18] L. A. Jackson, E. J. Anderson, N. G. Rouphael, P. C. Roberts, M. Makhene, R. N. Coler, M. P. McCullough, J. D. Chappell, M. R. Denison and L. J. Stevens, *An mRNA vaccine against SARS-CoV-2–preliminary report*, New England Journal of Medicine, 2020, 383(20), 1920–1931.

[19] S. Karlin, *A First Course in Stochastic Processes*, Academic Press, 2014.

[20] C. Li, J. Xu, J. Liu and Y. Zhou, *The within-host viral kinetics of SARS-CoV-2*, Mathematical Biosciences and Engineering, 2020, 17(4), 2853–2861.

[21] N. Louati, T. Rekik, H. Menif and J. Gargouri, *Blood lymphocyte T subsets reference values in blood donors by flow cytometry*, La Tunisie Medicale, 2019, 97(2), 327–334.

[22] C. Lucas, C. B. Vogels, I. Yildirim, J. E. Rothman, P. Lu, V. Monteiro, J. R. Gehlhausen, M. Campbell, J. Silva and A. Tabachnikova, *Impact of circulating SARS-CoV-2 variants on mRNA vaccine-induced immunity*, Nature, 2021, 600(7889), 523–529.

[23] S. Marino, I. B. Hogue, C. J. Ray and D. E. Kirschner, *A methodology for performing global uncertainty and sensitivity analysis in systems biology*, Journal of Theoretical Biology, 2008, 254(1), 178–196.

[24] F. Martinon, S. Krishnan, G. Lenzen, R. Magne, E. Gomard, J. G. Guillet, J. P. Lévy and P. Meulien, *Induction of virus-specific cytotoxic T lymphocytes in vivo by liposome-entrapped mRNA*, European Journal of Immunology, 1993, 23(7), 1719–1722.

[25] J. Mateus, J. M. Dan, Z. Zhang, C. R. Moderbacher, M. Lammers, B. Goodwin, A. Sette, S. Crotty and D. Weiskopf, *Low-Dose mRNA-1273 COVID-19 Vaccine Generates Durable Memory Enhanced by Cross-Reactive T Cells*, Science, 2021. DOI: 10.1126/science.abj9853.

[26] M. D. McKay, R. J. Beckman and W. J. Conover, *A comparison of three methods for selecting values of input variables in the analysis of output from a computer code*, Technometrics, 2000, 42(1), 55–61.

[27] H. Miao, X. Xia, A. S. Perelson and H. Wu, *On identifiability of nonlinear ODE models and applications in viral dynamics*, SIAM Review, 2011, 53(1), 3–39.

[28] H. Morbach, E. Eichhorn, J. Liese and H. Girschick, *Reference values for B cell subpopulations from infancy to adulthood*, Clinical and Experimental Immunology, 2010, 162(2), 271–279.

[29] M. J. Mulligan, K. E. Lyke, N. Kitchin, J. Absalon, A. Gurtman, S. Lockhart, K. Neuzil, V. Raabe, R. Bailey and K. A. Swanson, *Phase I/II study of COVID-19 RNA vaccine BNT162b1 in adults*, Nature, 2020, 586(7830), 589–593.

[30] S. L. Nutt, P. D. Hodgkin, D. M. Tarlinton and L. M. Corcoran, *The generation of antibody-secreting plasma cells*, Nature Reviews Immunology, 2015, 15(3), 160–171.

[31] F. P. Polack, S. J. Thomas, N. Kitchin, J. Absalon, A. Gurtman, S. Lockhart, J. L. Perez, G. PérezMarc, E. D. Moreira and C. Zerbini, *Safety and efficacy of the BNT162b2 mRNA COVID-19 vaccine*, New England Journal of Medicine, 2020, 383(27), 2603–2615.

[32] G. Regev-Yochay, T. Gonen, M. Gilboa, M. Mandelboim, V. Indenbaum, S. Amit, L. Meltzer, K. Asraf, C. Cohen and R. Fluss, *Efficacy of a fourth dose of COVID-19 mRNA vaccine against Omicron*, New England Journal of Medicine, 2022, 386(14), 1377–1380.

[33] R. F. Reis, A. B. Pigozzo, C. R. B. Bonin, B. D. M. Quintela, L. T. Pompei, A. C. Vieira, M. P. Xavier, R. W. Santos and M. Lobosco, *A validated mathematical model of the cytokine release syndrome in severe COVID-19*, Frontiers in Molecular Biosciences, 2021. DOI: 10.3389/fmolb.2021.639423.

[34] W. C. Roda, *Bayesian inference for dynamical systems*, Infectious Disease Modelling, 2020, 5(1), 221–232.

[35] N. Sugiura, *Further analysis of the data by Akaike's information criterion and the finite corrections: Further analysis of the data by Akaike's*, Communications in Statistics-theory and Methods, 1978, 7(1), 13–26.

[36] N. Tuncer, H. Gulbudak, V. L. Cannataro and M. Martcheva, *Structural and practical identifiability issues of immuno-epidemiological vector–host models with application to rift valley fever*, Bulletin of Mathematical Biology, 2016, 78(9), 1796–1827.

[37] Z. Yu, R. Ellahi, A. Nutini, A. Sohail and S. M. Sait, *Modeling and simulations of COVID-19 molecular mechanism induced by cytokines storm during SARS-CoV-2 infection*, Journal of Molecular Liquids, 2021. DOI: 10.1016/j.molliq.2020.114863.

[38] R. Yuan and Z. Wang, *A HIV infection model with periodic multidrug therapy*, Journal of Nonlinear Modeling and Analysis, 2019, 1(4), 573–593.

[39] Z. Zhang, J. Mateus, C. H. Coelho, J. M. Dan, C. R. Moderbacher, R. I. Gálvez, F. H. Cortes, A. Grifoni, A. Tarke and J. Chang, *Humoral and cellular immune memory to four COVID-19 vaccines*, Cell, 2022, 185(14), 2434–2451.